University of Applied Sciences Potsdam
Department of Conservation and Restoration

Science Laboratory

Church of the Virgin (Gelati)
Salt analyses – Part II

Potsdam, 25.07.2024

Prof. Dr. Steffen Laue
University of Applied Sciences Potsdam (FHP)
Kiepenheuerallee 5
D-14469 Potsdam
Tel.: +49-331-5804244
steffen.laue@fh-potsdam.de

Introduction

During the stay in the monastery complex in Gelati at the end of March 2024, in addition to the first series of samples (Laue 2024a), further salt efflorescence samples were taken at selected areas together with the restorers.

Additionally, depth profiles were drilled at four selected locations in order to determine the salt content of the drilling powder obtained.

Further additional efflorescence samples were sent to the laboratory in June 2024.

In addition to the salt investigations and the investigations by the colleagues from Italy, plaster samples were taken to determine the composition using XRD.

All analyses aim to better understand the origin of the salts, their distribution and their behavior.

Analytical methods

All samples and their sampling points were described and photographed in detail by Mariam Sagaradze, Lela Ninoshvili and colleagues in the restorers' documentation.

The efflorescences and crusts were observed with a Motic SMZ-160 stereo microscope, digital images were made with a Olympus DP28 digital camera on a BX51 microscope using dark field reflected light (DF).

The salts and plaster samples were analysed by using X-ray diffractometry (XRD): Empyrean X-ray diffractometer from Malvern Panalytical, operative conditions: CuKα radiation, 40KV, 40mA, 2Θ = 3-70°. Minerals with a concentration of approx. < 2% cannot be detected.

Due to a failure of the XRD, the salt sample S20 had to be analyzed by FTIR spectroscopy (PerkinElmer Spektrum 100) which also led to a clear result.

Drilling was carried out for quantitative salt ion analysis. The drill holes have a diameter of about 1 cm. First, the plaster layers were removed using a scalpel before drilling into the dolomitic stone. Drilling powder was obtained from various depths, from which soluble salt ions were subsequently extracted after drying as follows: 1 g of sample was mixed with 100 ml of distilled water. After a contact time of about 24 hours, the water with the dissolved salt ions were separated from the solid by filtration.
The electric conductivity (a value for the total amount of dissolved salt ions) and the pH value of the aqueous extracts were determined. Then, the extracts were analyzed using the ion chromatic system IC 90 (Thermo Fischer) after calibrating the chromatography system for the anions sulfate, nitrate, chloride and the cations potassium, sodium, calcium and magnesium. Data were calculated in weight percent (mass percent) [%w/w] and equivalent concentration [mEq/kg]. After conversion into equivalent concentration, all ions are equivalent in terms of weight and charge and can therefore be easily compared and evaluated with regard to concentration. The ion balance expresses the measured excess of cations in relation to the measured anions (cations minus anions).

Results

Efflorescences and crusts

The results of the salts measured by XRD (and one by FTIR) are summarized in Table 1 and are documented in the appendix 1.

After a total of 19 salt analyses from different surfaces in the main church, potassium nitrates in particular are frequently crystallized in addition to magnesium carbonates, magnesium sulfates and gypsum. Double salts such as picromerite or aphtitalite are less common – or they were not crystallized during sampling.

While the cause of the magnesium salts lies in the dolomite used as a building stone, the origin of the high concentrations of alkali ions is still unclear (see also the discussion after the quantitative analyses).

The salt on the painting in St. George's Church (S20) is magnesium sulfate, while in the NW chapel (S21 - S25) only magnesium salts and gypsum are present, no alkali salt so far.

Table 1: Sample ID, location, and results of the XRD measurements, (+): main salt, (-): to a lower degree, (=): present in approximately the same amount

Sample ID	Location	Crystallized Salts
S11	w arm S7	epsomite [$MgSO_4•7H_2O$] (+), hexahydrite [$MgSO_4•6H_2O$] (+), niter [KNO_3] (-)
S12	w arm N6	niter [KNO_3] (+), gypsum [$CaSO_4•2H_2O$] (-)
S13	s arm C12	epsomite [$MgSO_4•7H_2O$] (+), hexahydrite [$MgSO_4•6H_2O$] (+), gypsum [$CaSO_4•2H_2O$] (-)
S14	n arm W7	niter [KNO_3] (+), aphtitalite [$K_3Na(SO_4)_2$] (-)
S15	n arm W7	niter [KNO_3] (+), picromerite [$K_2Mg(SO_4)_2•6H_2O$] (-)
S16	n arm W7	niter [KNO_3]
S17	w arm W15	niter [KNO_3] = epsomite [$MgSO_4•7H_2O$] = hexahydrite [$MgSO_4•6H_2O$]
S18	n arm E5 Ne1/1	aphtitalite [$K_3Na(SO_4)_2$] (+), niter [KNO_3] (-)
S19	N arm W11 Nw1/1	niter [KNO_3] (+), aphtitalite [$K_3Na(SO_4)_2$] (-)
S20	St. Georg	epsomite [$MgSO_4•7H_2O$] and hexahydrite [$MgSO_4•6H_2O$] (FTIR)
S21	NWCh 5	dypingite [$Mg_5(CO_3)_4(OH)_2•5H_2O$] = lansfordite [$MgCO_3•5H_2O$]
S22	NWCh N10	epsomite [$MgSO_4•7H_2O$] (+), gypsum [$CaSO_4•2H_2O$] (-)
S23	NWCh Icono.	gypsum [$CaSO_4•2H_2O$]
S24	NWCh S7	hydromagnesite [$Mg_5(CO_3)_4(OH)_2•4H_2O$]
S25	N-entrance W5	calcite [$CaCO_3$] (+),gypsum [$CaSO_4•2H_2O$] (-)

Quantitative salt analyses

Depth profiles were drilled at four selected locations in order to determine the salt content in depth:

1) Ne1: North arm, east wall, Scene E9, Height from floor level: 16,7 m; 0,5 m from north wall.

2) Ne2: North arm, east wall, Scene E7, Height from floor level: 13,4 m; 0,6 m from north wall.

3) Ne3: North arm, east wall, Scene E5, Height from floor level: 7,8 m; 0,7 m from north wall.

4) Nw1: North arm, west wall, Scene W11, Height from floor level: 12,1 m; 0,9 m from north wall.

All data are documented in detail in appendix 2.

Fig. 1 to 5 attempt to illustrate the key results.

From Fig. 1 it is clear that a heterogeneous salt ion distribution can be observed at different heights in the north arm on the east wall, with the salt ions being enriched particularly in the plaster layers at the front, while significantly fewer salt ions are found in the dolomite stone.

Looking at all depth profiles in detail (Fig. 2 to 5), it is noticeable that three of four profiles are very different, and only Ne3 is similar to profile Nw1, although the alkali contents in the two samples differ significantly.

In addition to the heterogeneous salt distribution, the high cation excess in the front cm at the locations Ne1, Ne2 and Nw1 is particularly noticeable. This demonstrates that at least one important anion was not detected in the analyses.

Further analyses using another chromatograph from a cooperating institute showed that the unknown anion is oxalate. Alkali oxalates are obviously present in the surfaces examined so far, but have not yet been detected as efflorescence salts. The oxalate content in the surfaces still needs to be quantified. And the question arises, where do the soluble oxalates come from?

In the profiles Ne3 and Nw1, high concentrations of potassium, sodium, nitrate and sulfate are noticeable in the plaster. Calcium and magnesium play no role here, although dolomite rock is present in the background.

Due to the high alkali content, the urgent question arises: What is the source of the salt ions of the alkalis sodium and potassium. Were areas possibly treated with a conservation material that contains alkalis?

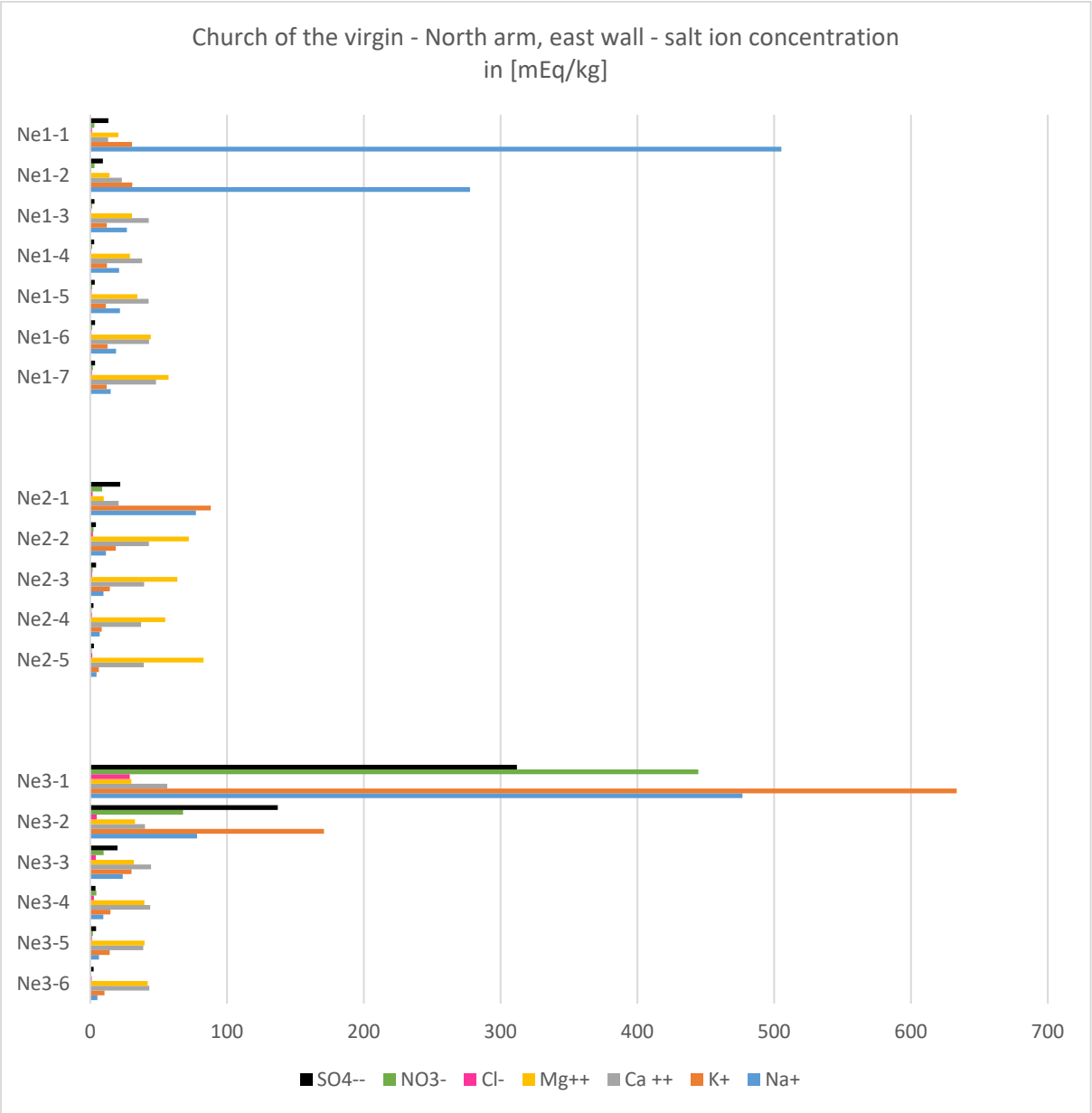

Fig. 1: Overview of the salt ion distribution in the north arm on the east wall in height and depth profiles. The highest concentration shown at each height is the foremost depth (Nex-1), then further down follow the other depths.

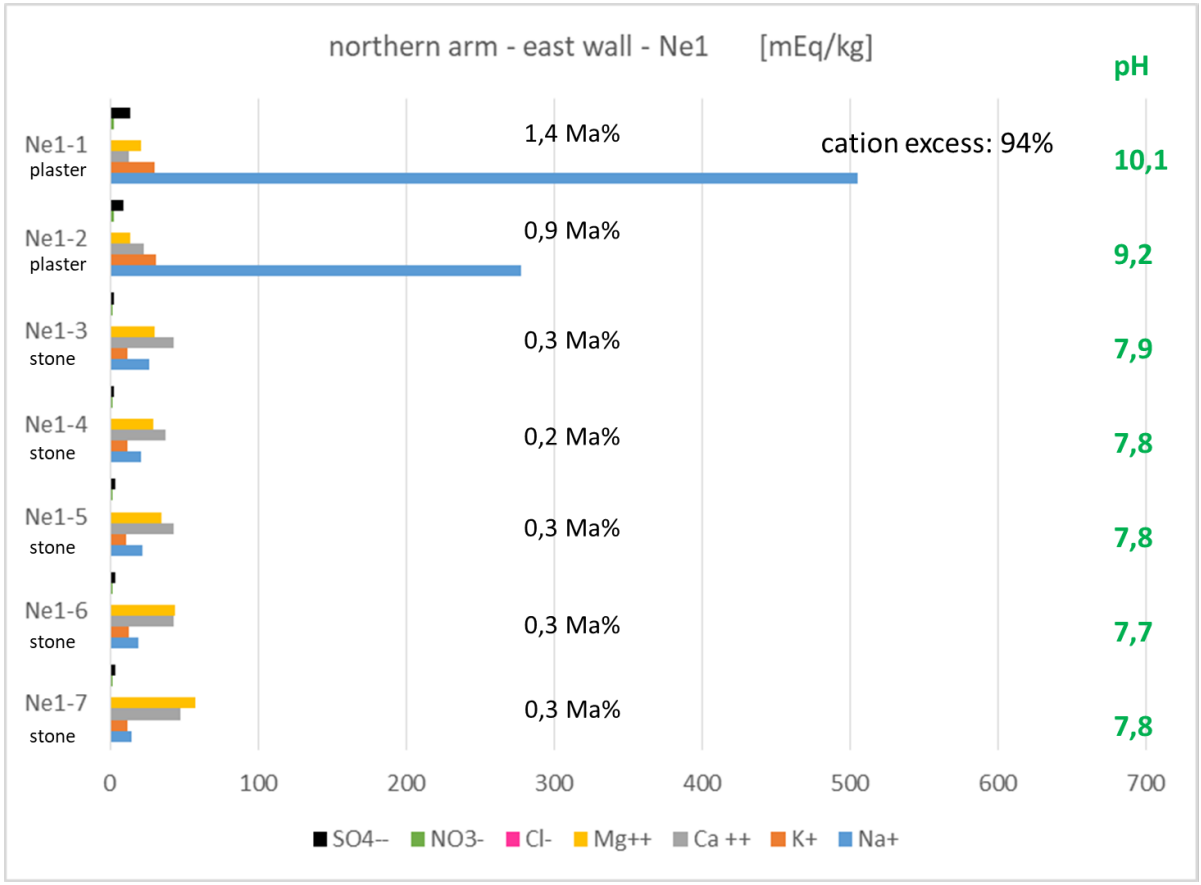

Fig. 2: Salt ion distribution in the depth profile at the location Ne1, starting at the top with the first depth, salt ion concentration is shown in color in the unit [mEq/kg]. In addition, the total ion content of the respective depth is given in mass percent and the cation excess in the first depth, on the right in green the pH value of the water extract. The extreme excess of cations (here sodium) is evident, most of the anions were not detected in this measurement.

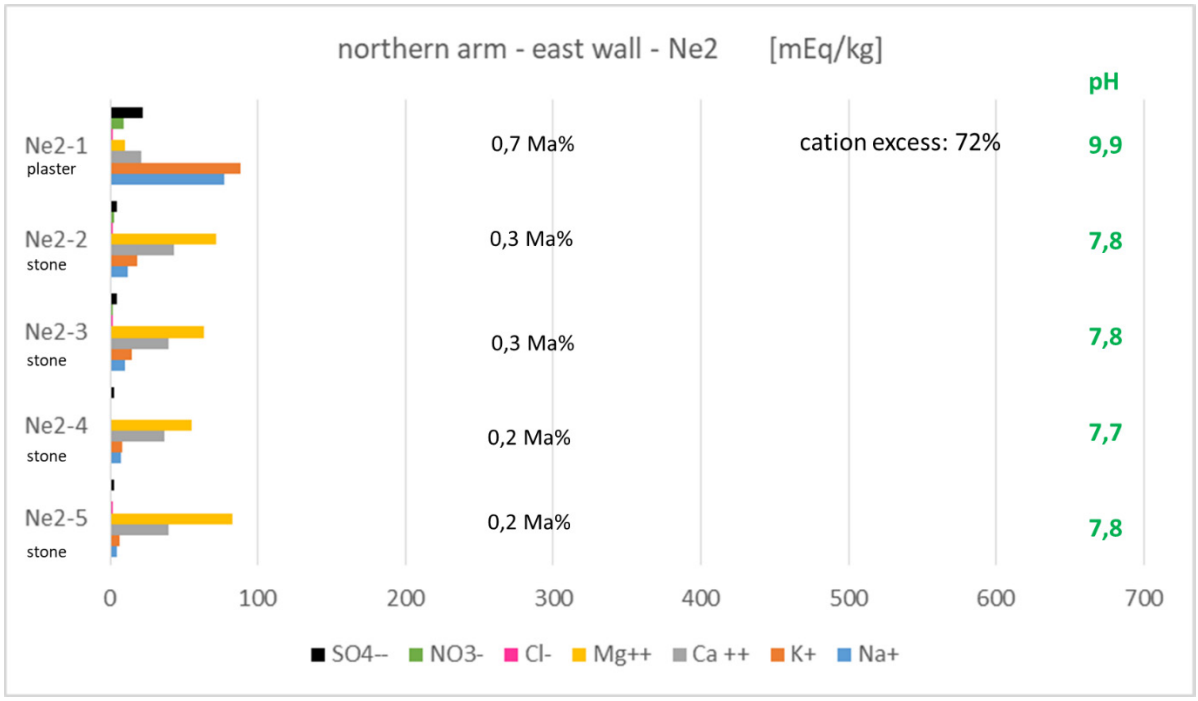

Fig. 3: Salt ion distribution in the depth profile at the location Ne2, explanation see Fig. 1. In this area of the wall the overall salt content is low

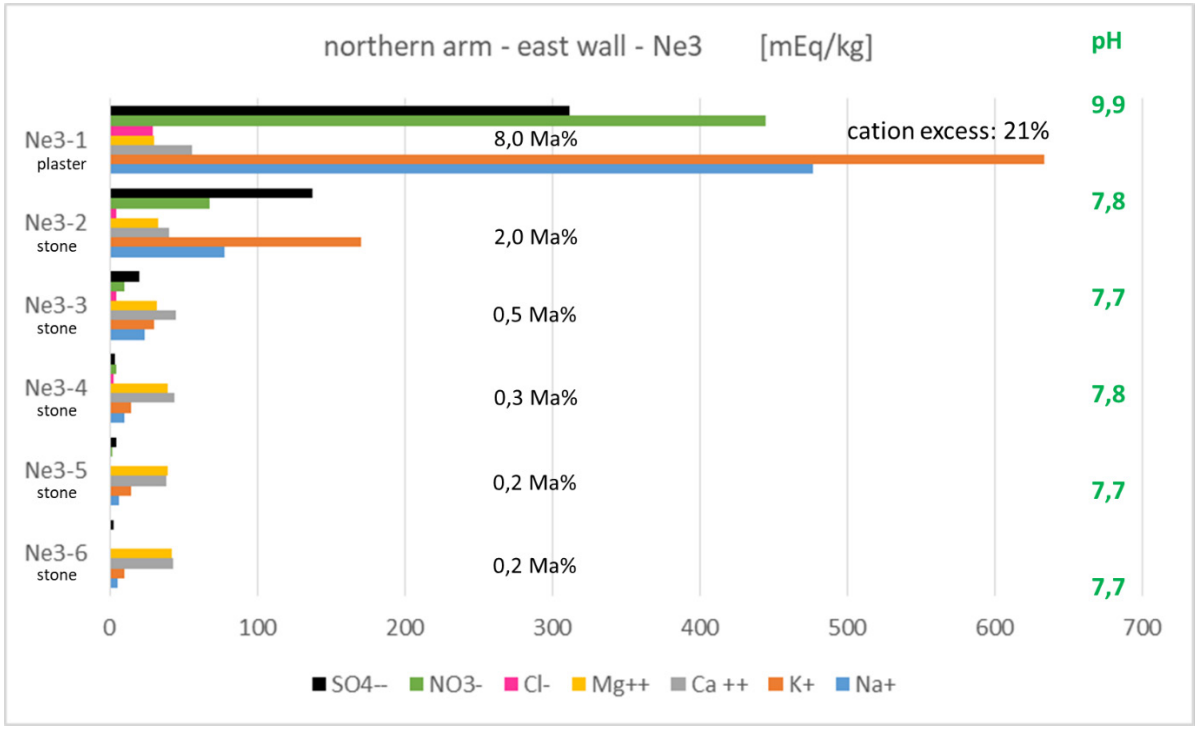

Fig. 4: Salt ion distribution in the depth profile at the location Ne3, explanation see Fig. 1. The salt content in the plaster is very high and the cation excess of about 20% is plausible, since the anion carbonate is not measurable and dolomite stone is in the background.

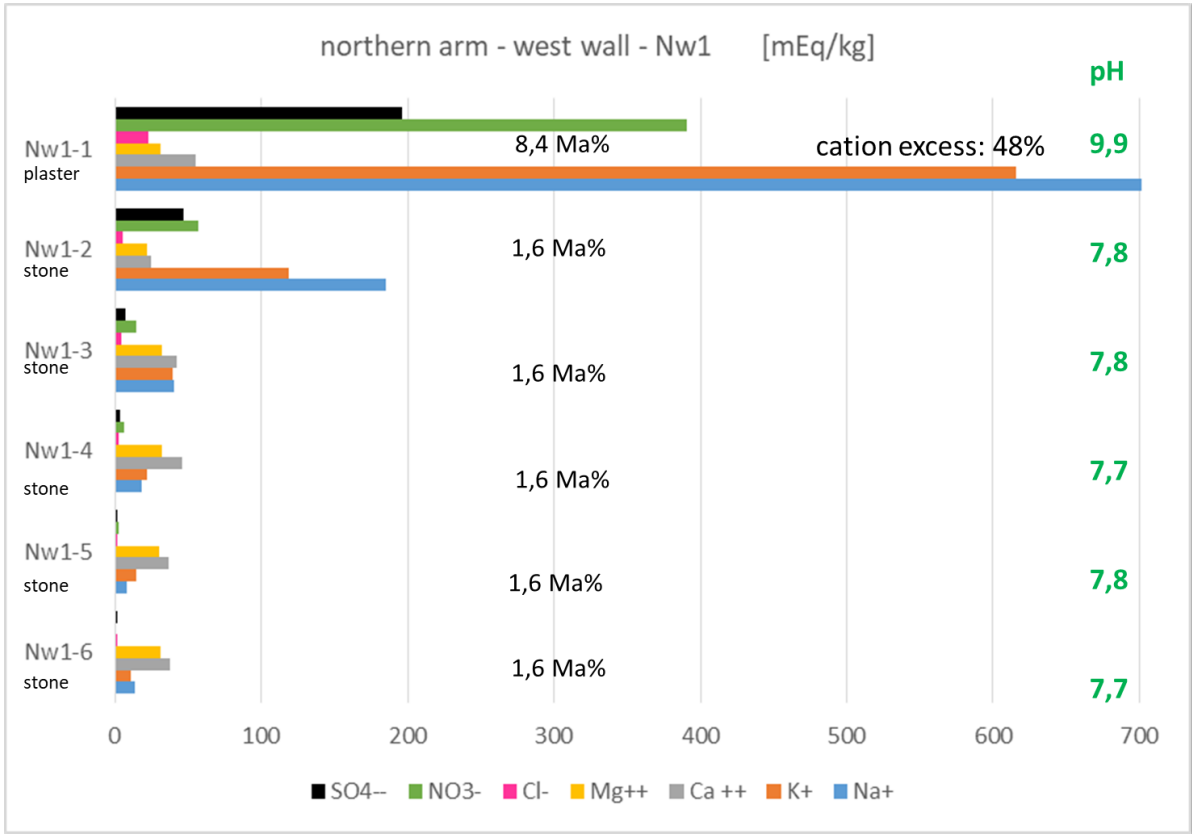

Fig. 5: Salt ion distribution in the depth profile at the location Nw1, explanation see Fig. 1. The salt content in the plaster is very high. Here, the cation excess is too high at about 50%, which means that an important anion was not detected in the analysis. As with location Ne1, there is also a high proportion of sodium here, and an overall high alkali content.

Plaster analyses by XRD

Two different, relatively thin layers of plaster could be distinguished on the stone surfaces in the church as supports for wall paintings (see also illustrations in Appendix 3):

1. fine-grained white plaster with visible straw-like components.

2. fine-grained white plaster with conspicuous dark aggregate surfaces.

It should be clarified whether magnesium-containing components are contained in the plaster.

Table 2 gives an overview of the samples examined so far and the results; further details can be found in the appendix 3.

Table 2: Plaster samples and results by XRD (appendix 3)

Sample	plaster type	
Sw_Pl_2.1, W8	with straw-like components	Dolomite > Calcite = quartz
Sw_Pl_2-2, W8	with black aggregates	Calcite > Dolomite = quartz
Ne2_1, E7	with black aggregates	Calcite > Dolomite = quartz
Nw1_1	with black aggregates	Calcite > Dolomite = quartz

The results of the plaster analyses have shown so far that both types of plaster differ in their dolomite and calcite content. While the plaster with the straw-like components has a high dolomite content, only a small amount of dolomite can be detected in the plaster with the black additives.

Since only dolomite and no other magnesium carbonates can be analyzed, it can be assumed that both plasters are lime plasters and contain dolomite as an additive.

Further plaster analyses are still being carried out.

Summary and discussion

The results so far have shown that, in addition to some gypsum, at least three main different salt systems in particular contribute to the damage in the Church of the Virgin:

1. Magnesium carbonate

2. Magnesium sulfate

3. Potassium nitrate

In addition, in some samples, double salts with two cations and sulfate could also be detected (aphtitalite, picromerite and syngenite), which indicates the complexity of the salt ion mixtures in at least some areas of the walls.

All salts have different behavior depending on the solubility properties, the respective deliquescence humidities and whether they can hydrate and dehydrate (detailed information see www.saltwiki.net).

Although the salt ion contamination in the church is heterogeneously distributed and different salt ion mixtures occur in different quantities, the following damage scenarios are conceivable based on the qualitative and quantitative salt analyses so far.

The building stone of the church is made of dolomite stone, which consists mainly of the mineral dolomite [$MgCa(CO_3)_2$]. Dolomite was also found in at least two plastering phases. The use of dolomite-lime mortar in the church cannot be ruled out either. Dolomite is a poorly soluble mineral (www.saltwiki.net), but due to moisture ingress over a long period of time, dolomite compo-

nents were dissolved, ions were transported and after drying, magnesium carbonate and magnesium carbonate hydrate phases are crystallizing, such as the minerals (salts) magnesite [$MgCO_3$], hydromagnesite [$Mg_5(CO_3)_4(OH)_2•4H_2O$], nesquehonite [$MgCO_3•3H_2O$], lansfordite [$MgCO_3•5H_2O$] and dypingite [$Mg_5(CO_3)_4(OH)_2•5H_2O$], which we find today in and on the surfaces of the church.

If, in addition to these magnesium carbonate minerals, a sulphate source is added, for example through gypsum supplements used or through anthropogenic pollutant gases, which in earlier years probably existed for long periods in the city of Kutaisi and were also transported to rural areas by winds, magnesium sulphates such as epsomite [$MgSO_4•7H_2O$] and hexahydrite [$MgSO_4•6H_2O$] are formed after moisture ingress and drying, both of which have been detected on various surfaces of the church. Magnesium sulfates are more soluble than magnesium carbonates and have the additional damaging property of hydrating and dehydrating depending on relative humidity variations. At higher relative humidities, epsomite is the stable phase, while at lower humidities hexahydrite is most likely present. This means that the two salts convert into each other depending on the climate. The crystal lattice collapses briefly and then the new phase crystallizes with corresponding volume changes and damage to the porous system. Although we do not know the exact climatic conditions under which the transformation takes place (it depends, among other things, on temperature, relative humidity, ion composition of the ion mixture prevailing on the surface), it is in any case advisable to reduce magnesium sulfate ions from the surface area in order to avoid the hydration and dehydration processes of this special salt system.

Sulfate ions present on surfaces frequently react with calcium ions, which are always found in buildings, to form the poorly soluble mineral gypsum [$CaSO_4•2H_2O$]. Gypsum only dissolves when there is a film of moisture on a surface, which is the case in the church due to water ingress and possibly also due to condensation events.

In addition, the quantitative salt analyses of all measured surfaces show a high alkali content of sodium and potassium as well as a high pH value in the plasters, the reasons for this have not yet been clarified. In addition to the salts with two cations syngenite [$K_2Ca(SO_4)_2•H_2O$], aphtitalite [$K_3Na(SO_4)_2$] and picromerite [$K_2Mg(SO_4)_2•6H_2O$], we find often niter [KNO_3] above all as an efflorescence salt. Niter has the special property that its solubility is strongly temperature-dependent: at high temperatures, niter is highly soluble, but at cold temperatures the solubility is greatly reduced, which leads to crystallization preferably at cold temperatures and has led to an increased damage process in winter months analyzed in several monuments (Laue 2006, Laue 2023).

In addition, the high sodium content and the excess of cations in the front cm of the walls in the church are noticeable in respect to the analyzed ions. The excess of cations can be explained by the anions oxalate and carbonate, which are not included in the ion balance. Oxalate has been detected but not yet quantified, and carbonates cannot be measured using IC.

Although there is a lot of sodium in the surfaces, hardly any crystallized sodium salts have been found so far. However, they represent a salt ion potential that can become damagingly active when climatic conditions change. Since all sodium salts are high soluble, salt reduction measures could help to improve the situation.

Outlook

The damage scenarios presented should be verified or falsified by targeted monitoring: For each of the crystallized salt systems (magnesium carbonate, magnesium sulfate and potassium nitrate) and the surfaces containing oxalate and sodium, at least two (or more) different reference areas cleaned of salts should be created in different areas of the church. In combination with the climate data, it should be determined when which new crystallizations can be detected and under which climatic conditions – following the approaches of Andreas Arnold and colleagues, who have successfully applied this method to many monuments (Arnold & Zehnder 1991).

Salt reduction can be generally successful, as the strong salinization is only in the plaster layers and not in the underlying stone. By understanding the salt activities, it is also possible to find an optimized time for reducing a corresponding salt.

The reason for the high alkali content in the surfaces should be determined. Were the wall paintings possibly treated at any time with an alkaline conservation material that contains alkalis?

In addition, the quantitative salt analyses have shown how heterogeneously the wall sections of the church are contaminated with salt ions. It is recommended that the salt contamination should be analyzed before each section of wall painting will be preserved. The analyses have shown that only the plaster materials need to be analyzed for this purpose; the stone in the background is relatively dense and only contains the stone's own ions calcium, magnesium and carbonate, which - once the moisture ingress has been stopped - probably remain in the stone.

References

Arnold, A. & Zehnder, K. (1991): Monitoring wall paintings affected by soluble salt.- The Conservation of Wall Paintings, Sympos. by Courtauld Inst. of Art at the Getty Conserv. Inst., London, July 13-16, 1987, 103-135.

Laue, S. (2005): Salt Weathering of Porous Structures Related to Climate Changes.- Restoration of Buildings and Monuments, vol. 11, No. 6, pp. 381-390, 2005.

Laue, S. (2023): Monitoring as a basic tool for understanding salt crystallization processes on monuments – case study of the baroque tomb in St. Marien in Frankfurt/Oder.- In: Abuku, M. & Takatori, N. (ed.): Saltweathering on Buildings and Stone Sculptures, SWBSS ASIA 2023, September 20-22, 2023, Nara, Japan, 75-84.

Laue, S. (2024): Church of the Virgin (Gelati) – Salt analyses Part I.- unpublished report, 20.03.2024, 14 pages.

Stephen, H & Stephen, T. (1963): Solubilities of inorganic and organic compounds, Pergamon Press, Oxford, p. 116, p 180.

www.saltwiki.net

Appendix I

Documentation of the measurements of salt efflorescences and crusts

Sample 11 – Location: West arm, south wall, IV register, S7

Description: transparent short columnar crystals (whisker) (DF) (Fig. I-1).

Result by XRD: mostly epsomite [$MgSO_4 \cdot 7H_2O$] and hexahydrite [$MgSO_4 \cdot 6H_2O$] and to a much lower degree niter [KNO_3] and gypsum [$CaSO_4 \cdot 2H_2O$] (Fig. I-2).

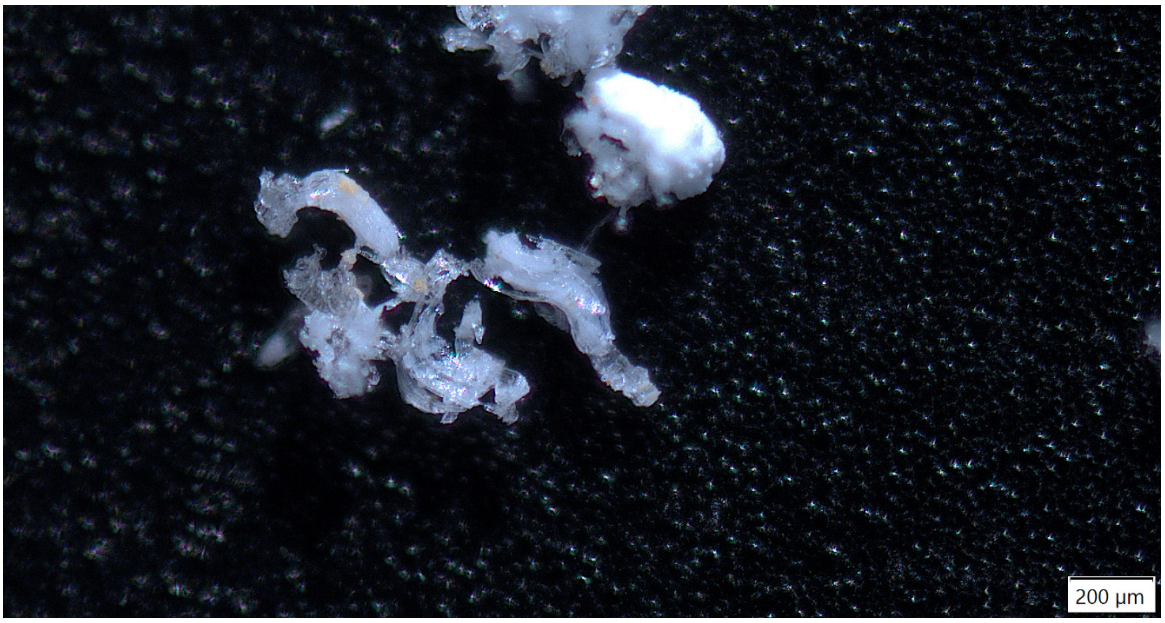

Fig. I-1: Sample 11

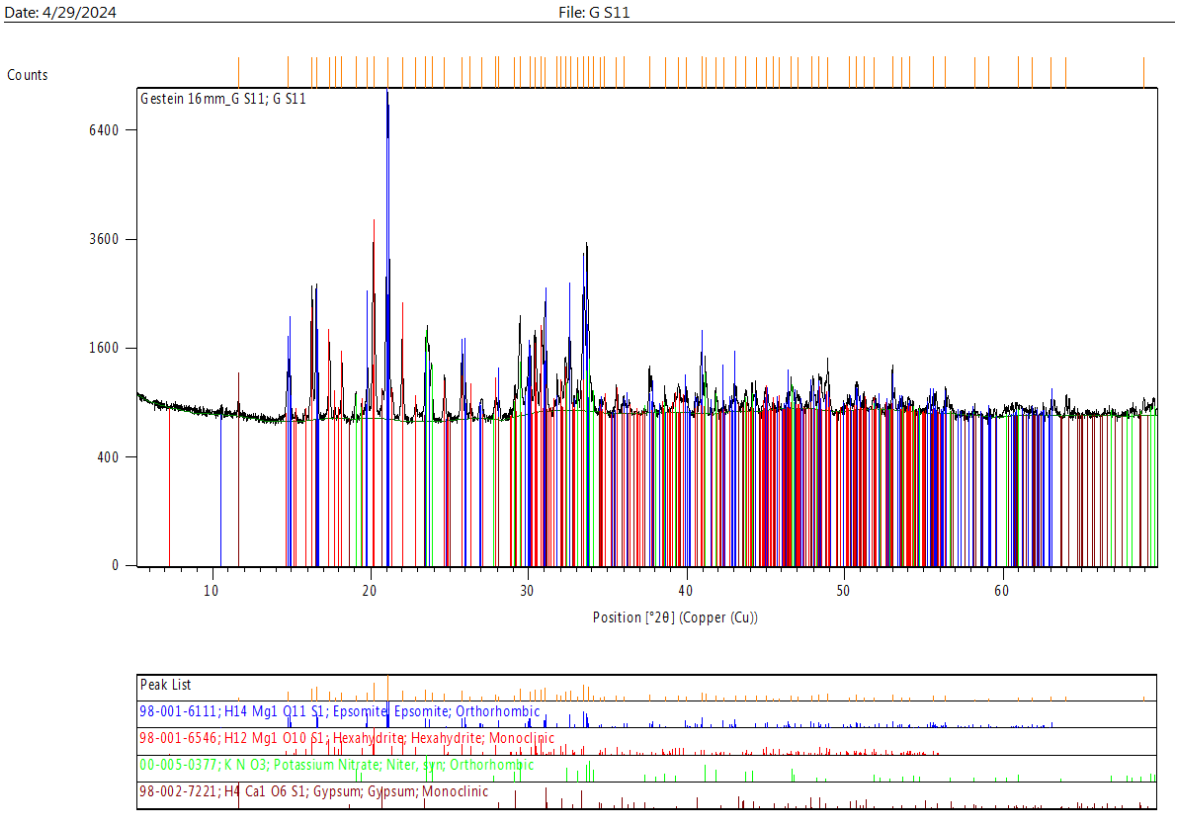

Fig. I-2: Sample 11, XRD spectrum

Appendix I

Documentation of the measurements of salt efflorescences and crusts

Sample 12 – Location: West arm, north wall, IV register, N6

Description: granular crystals agglomerated to a crust (Fig. I-3).

Result by XRD: mostly niter [KNO_3] and to a much lower degree gypsum [$CaSO_4 \cdot 2H_2O$] (Fig.I-4).

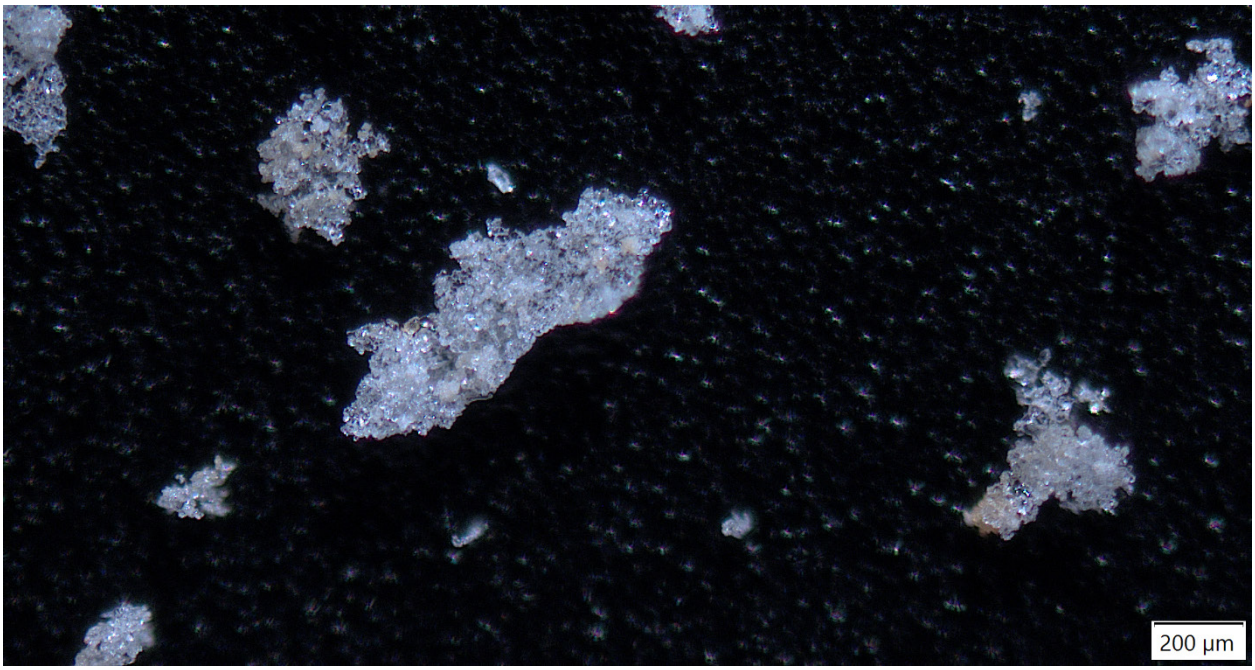

Fig. I-3: Sample 12: granular crystals agglomerated to a crust

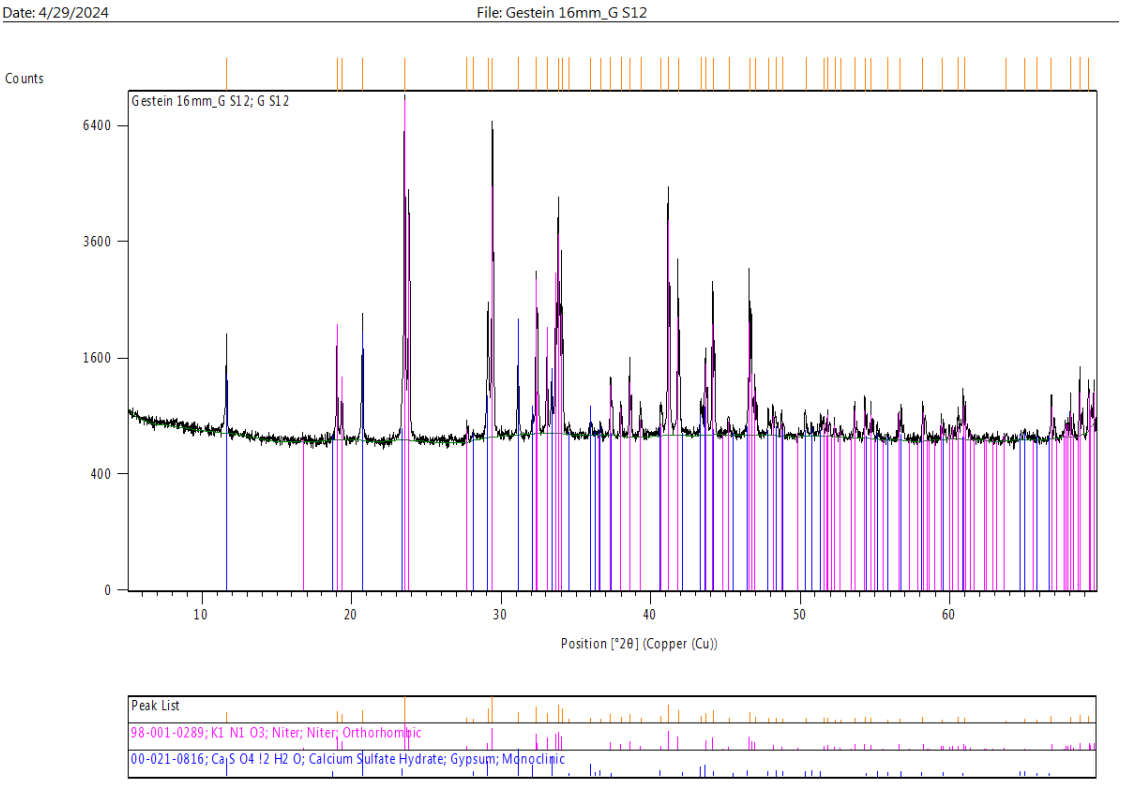

Fig. I-4: Sample 12, XRD spectrum

Appendix I

Documentation of the measurements of salt efflorescences and crusts

Sample 13 – Location: South Arm, vault, C12

Description: white crust with blue particles (Fig. I-5).

Result by XRD: mostly epsomite [$MgSO_4 \cdot 7H_2O$] and hexahydrite [$MgSO_4 \cdot 6H_2O$] and to a lower degree gypsum [$CaSO_4 \cdot 2H_2O$] (Fig. I-6).

Fig. I-5: Sample 13: white crust with blue particles

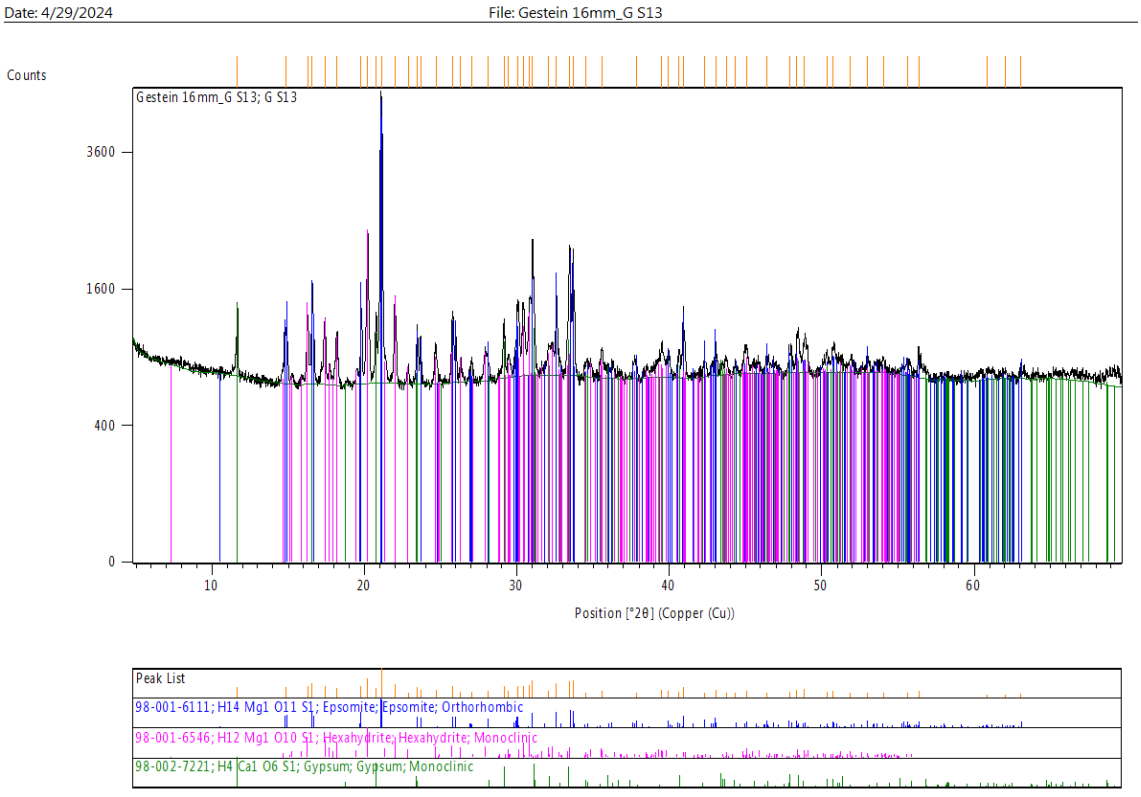

Fig. I-6: Sample 13, XRD spectrum

Appendix I

Documentation of the measurements of salt efflorescences and crusts

Sample 14 – Location: North Arm, West wall, IV register, W7

Description: transparent whisker (Fig. I-7).

Result by XRD: mostly niter [KNO_3] and to a much lower degree aphtitalite [$K_3Na(SO_4)_2$] (Fig.I-8).

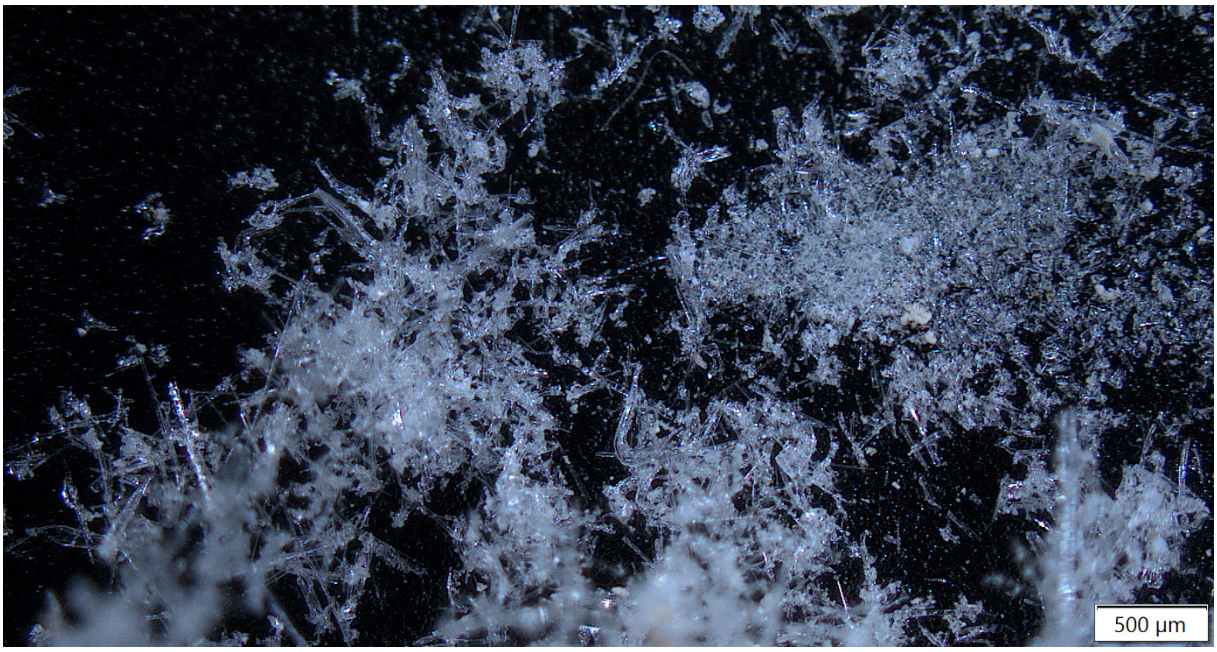

Fig. I-7: Sample 14: transparent whisker

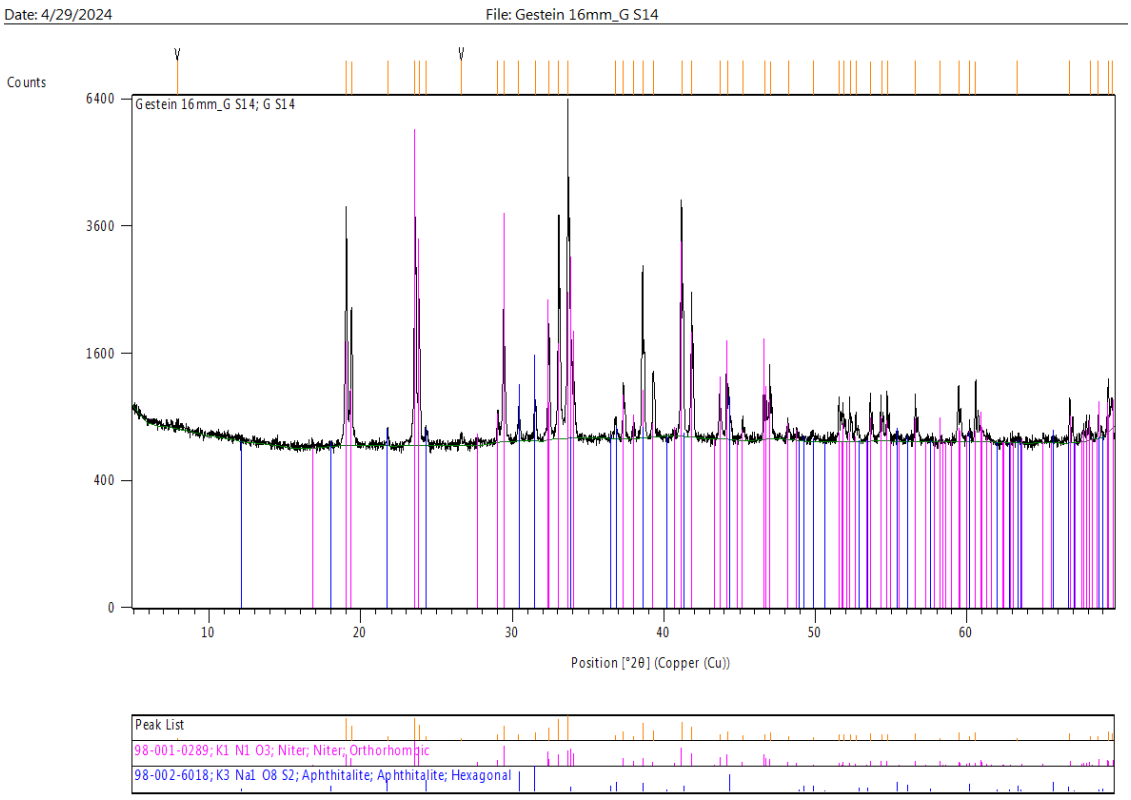

Fig. I-8: Sample 14, XRD spectrum

Appendix I

Documentation of the measurements of salt efflorescences and crusts

Sample 15 – Location: North Arm, West wall, IV register, W7

Description: granular crystals agglomerated to a white crust (Fig. I-9).

Result by XRD: mostly niter [KNO_3] and to a much lower degree picromerite [$K_2Mg(SO_4)_2 \cdot 6H_2O$] (Fig.I-10).

Fig. I-9: Sample 15: granular crystals agglomerated to a white crust

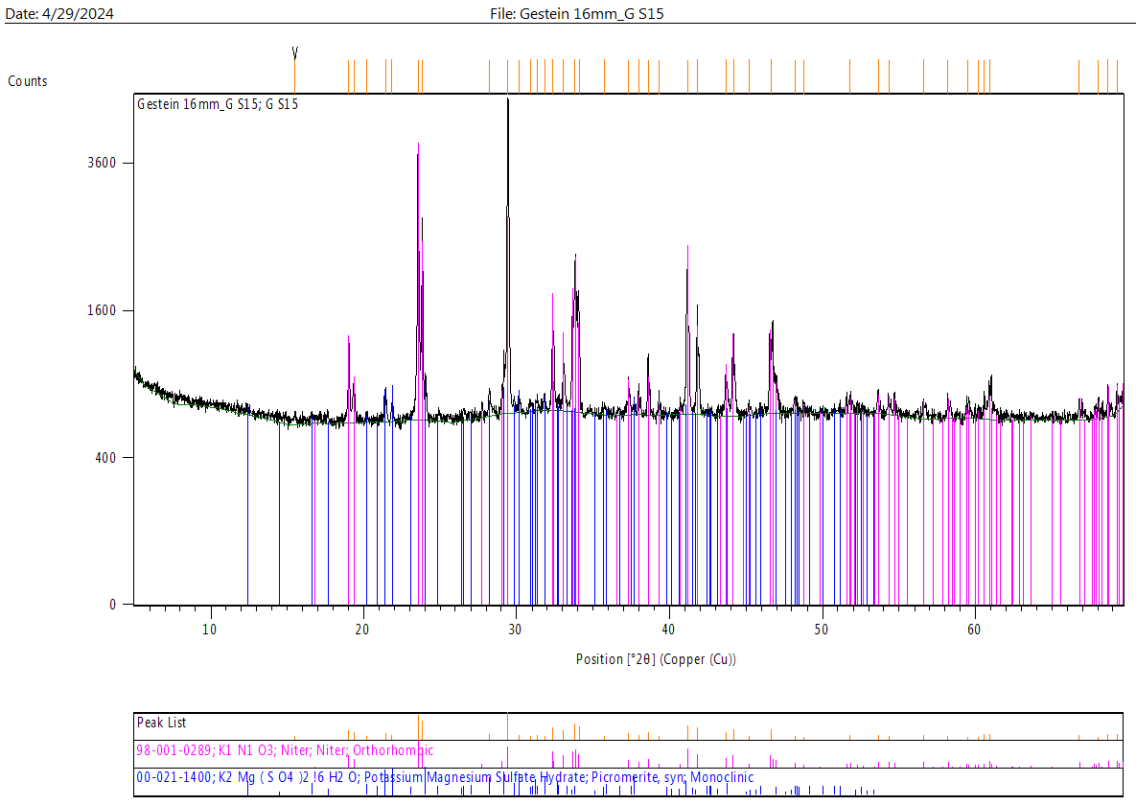

Fig. I-10: Sample 15, XRD spectrum

Appendix I

Documentation of the measurements of salt efflorescences and crusts

Sample 16 – Location: North Arm, West wall, IV register, W7

Description: granular crystals agglomerated to a crust with ochre particles (Fig. I-11).

Result by XRD: niter [KNO_3] (Fig.I-12).

Fig. I-11: Sample 16: granular crystals agglomerated to a crust with ochre particles

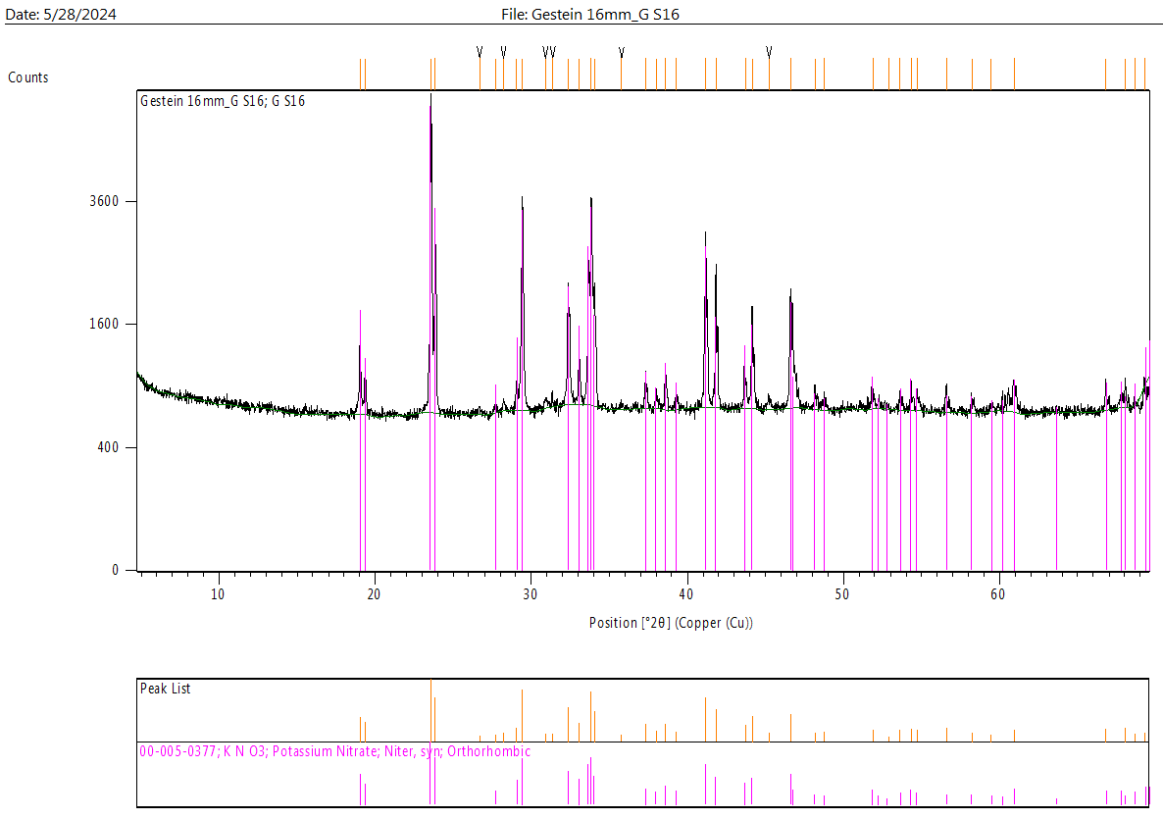

Fig. I-12: Sample 16, XRD spectrum

Appendix I

Documentation of the measurements of salt efflorescences and crusts

Sample 17 – Location: West Arm, West wall, W15

Description: white crust (Fig. I-13).

Result by XRD: niter [KNO_3] in the same quantity as epsomite [$MgSO_4 \cdot 7H_2O$] and hexahydrite [$MgSO_4 \cdot 6H_2O$] (Fig. I-14).

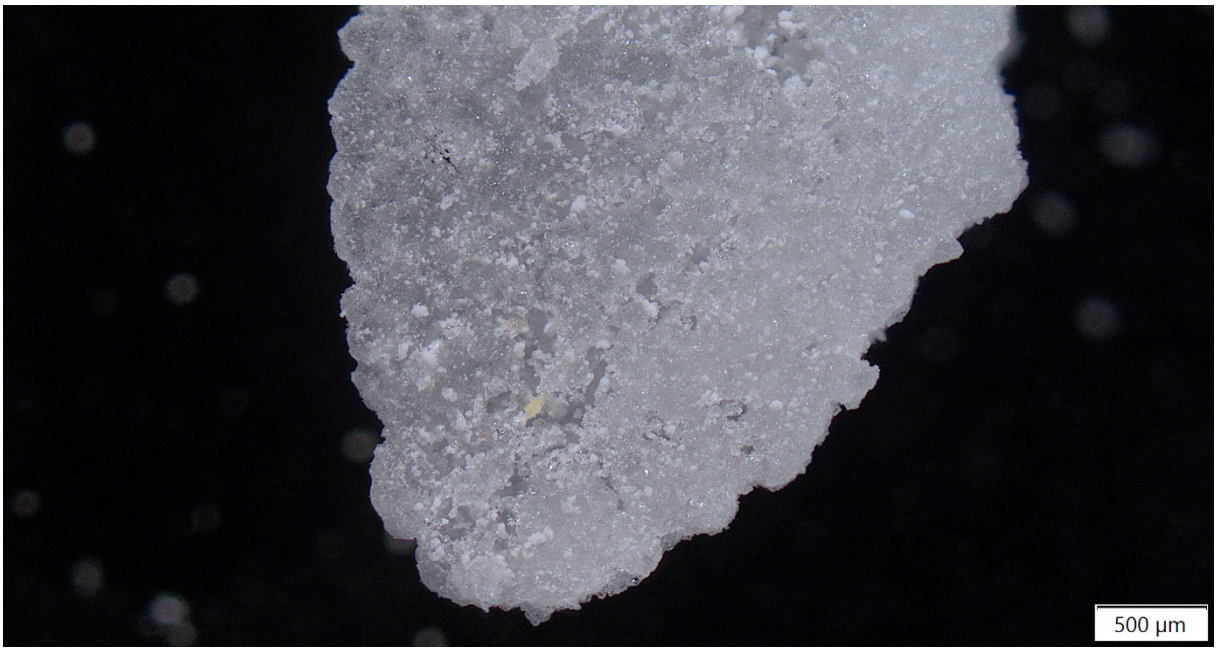

Fig. I-13: Sample 17: white crust

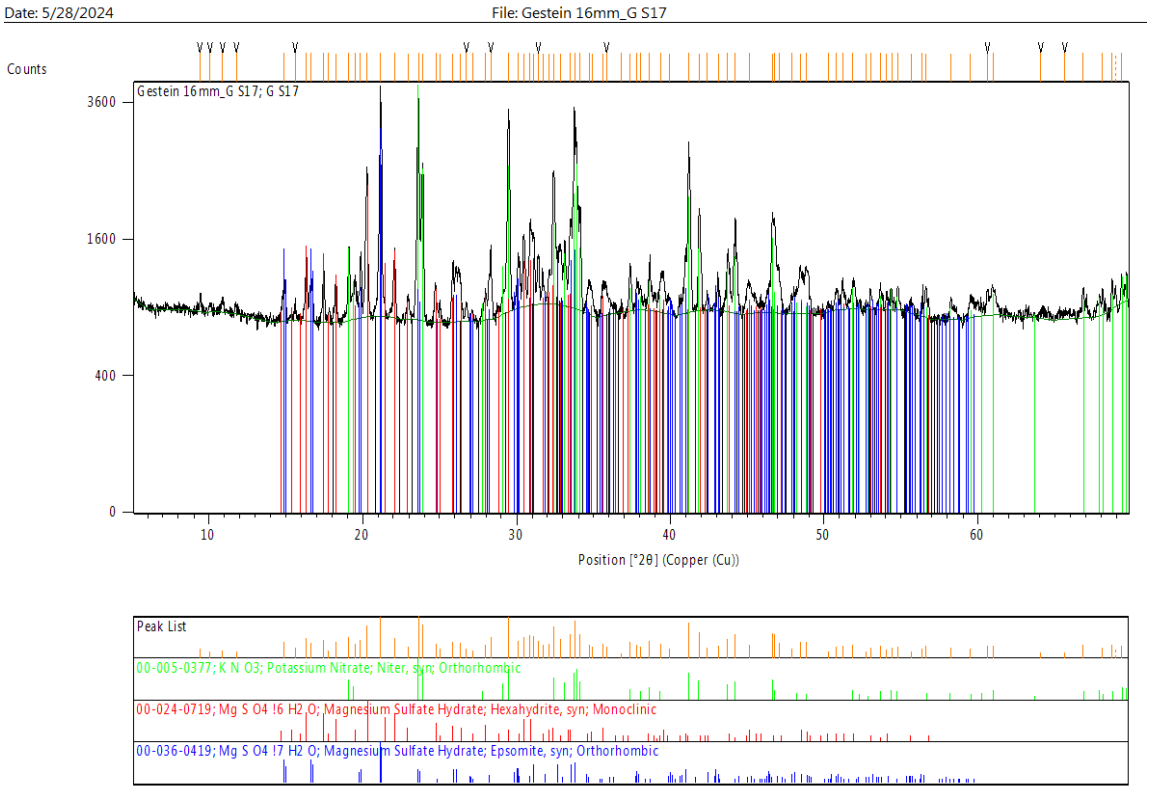

Fig. I-14: Sample 17, XRD spectrum

Appendix I

Documentation of the measurements of salt efflorescences and crusts

Sample 18 – Location: North Arm, East wall, E5

Description: thin white crusts and transparent granular crystals agglomerated to a crust (Fig. I-15).

Result by XRD: mostly aphtitalite [$K_3Na(SO_4)_2$] and to a much lower degree niter [KNO_3] (Fig. I-16).

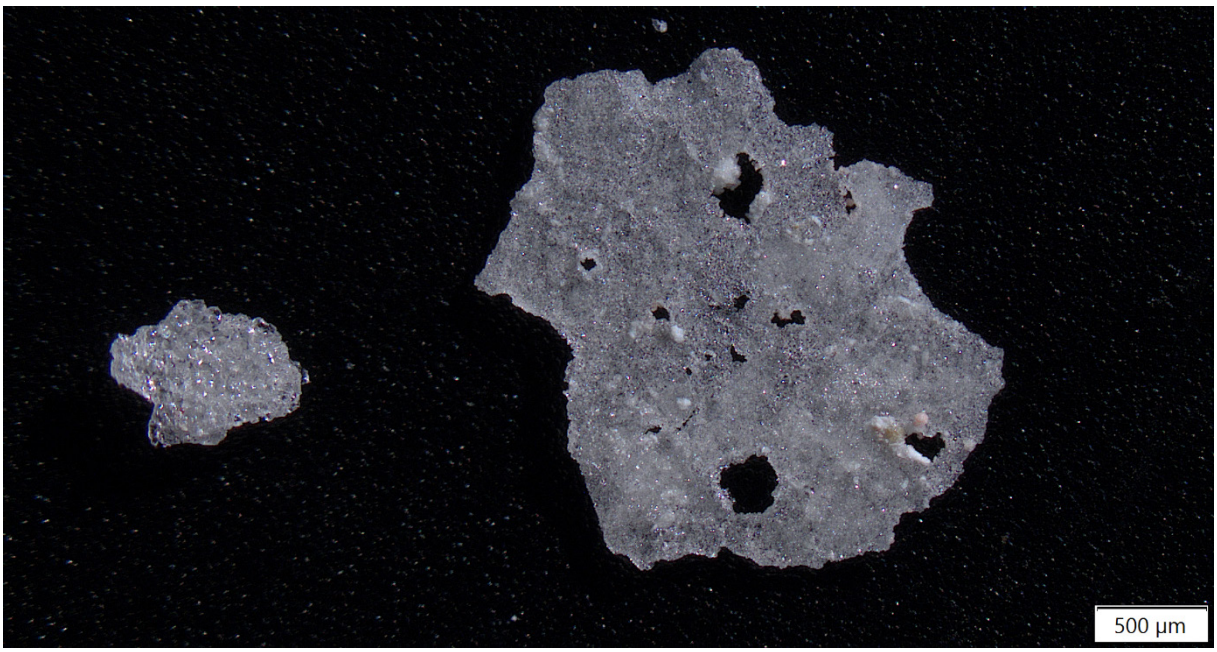

Fig. I-15: Sample 18: thin white crusts and transparent granular crystals agglomerated to a crust

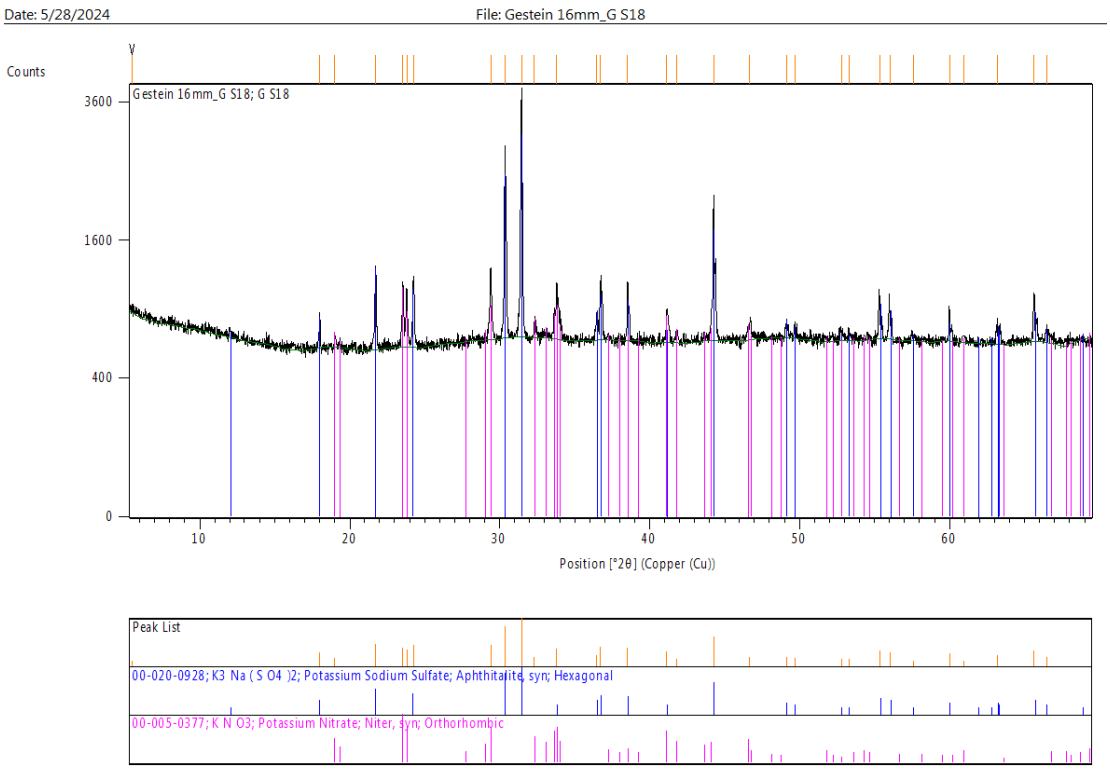

Fig. I-16: Sample 18, XRD spectrum

Appendix I

Documentation of the measurements of salt efflorescences and crusts

Sample 19 – Location: North Arm, west wall, W11

Description: transparent whisker, partly agglomerated (Fig. I-17).

Result by XRD: mostly niter [KNO_3] and to a much lower degree aphtitalite [$K_3Na(SO_4)_2$] (Fig. I-18).

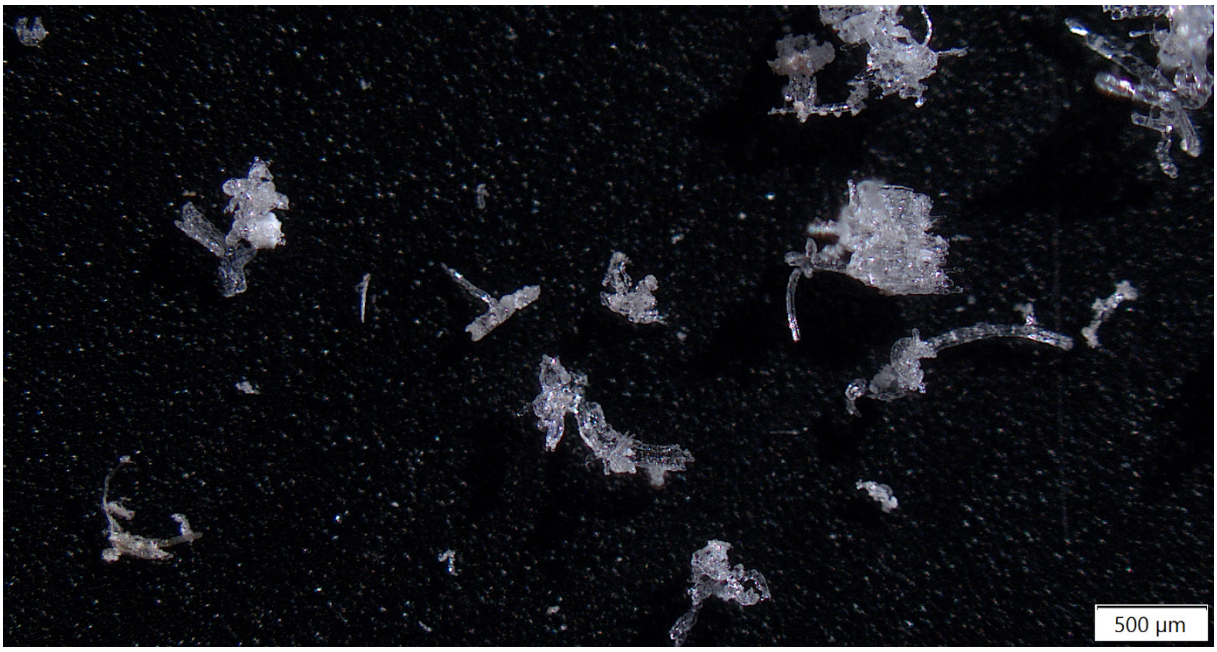

Fig. I-17: Sample 19: transparent whisker, partly agglomerated

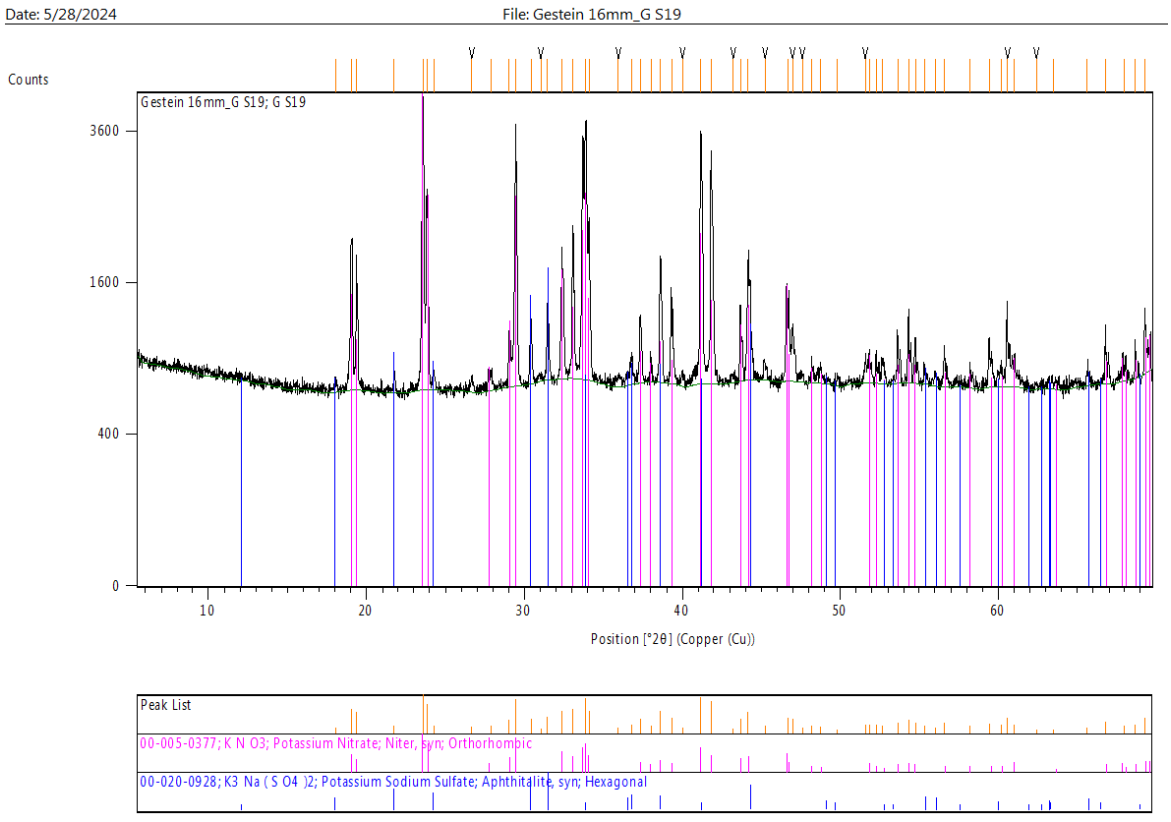

Fig. I-18: Sample 19, XRD spectrum

Appendix I

Documentation of the measurements of salt efflorescences and crusts

Sample 20 – Location: St. George, North wall, Donor

Description: white crusts and transparent whisker (Fig. I-19).

Result by FTIR: epsomite [$MgSO_4 \cdot 7H_2O$] and hexahydrite [$MgSO_4 \cdot 6H_2O$] (Fig. I-20).

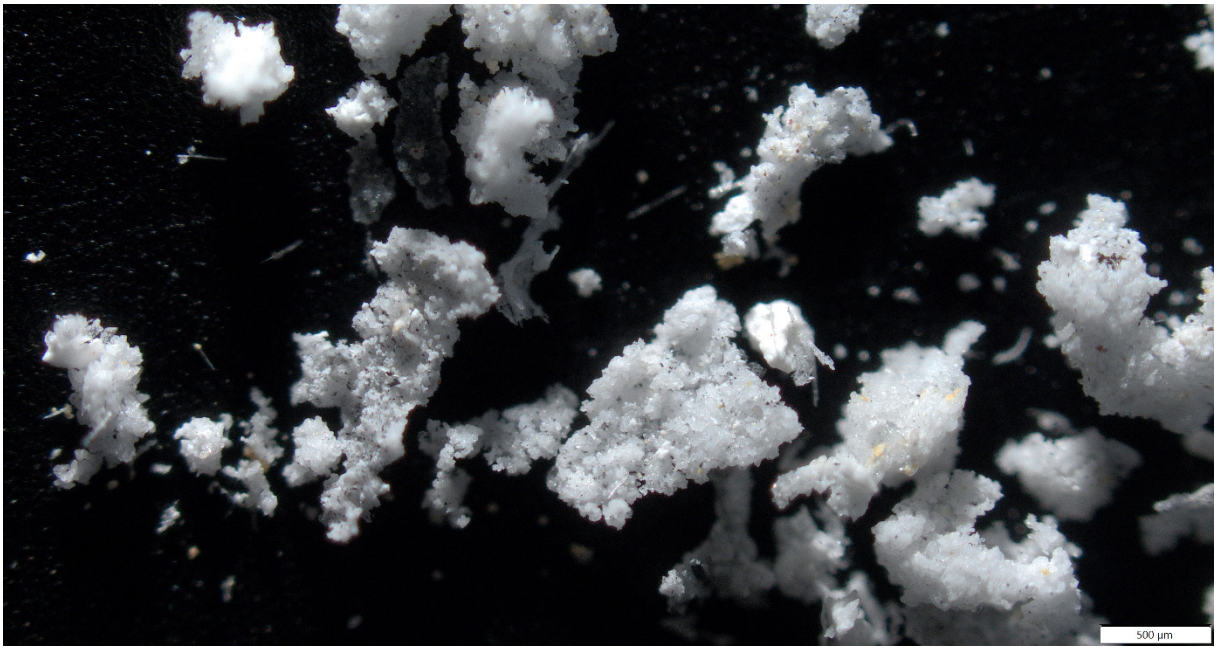

Fig. I-19: Sample 20: white crusts and some whisker

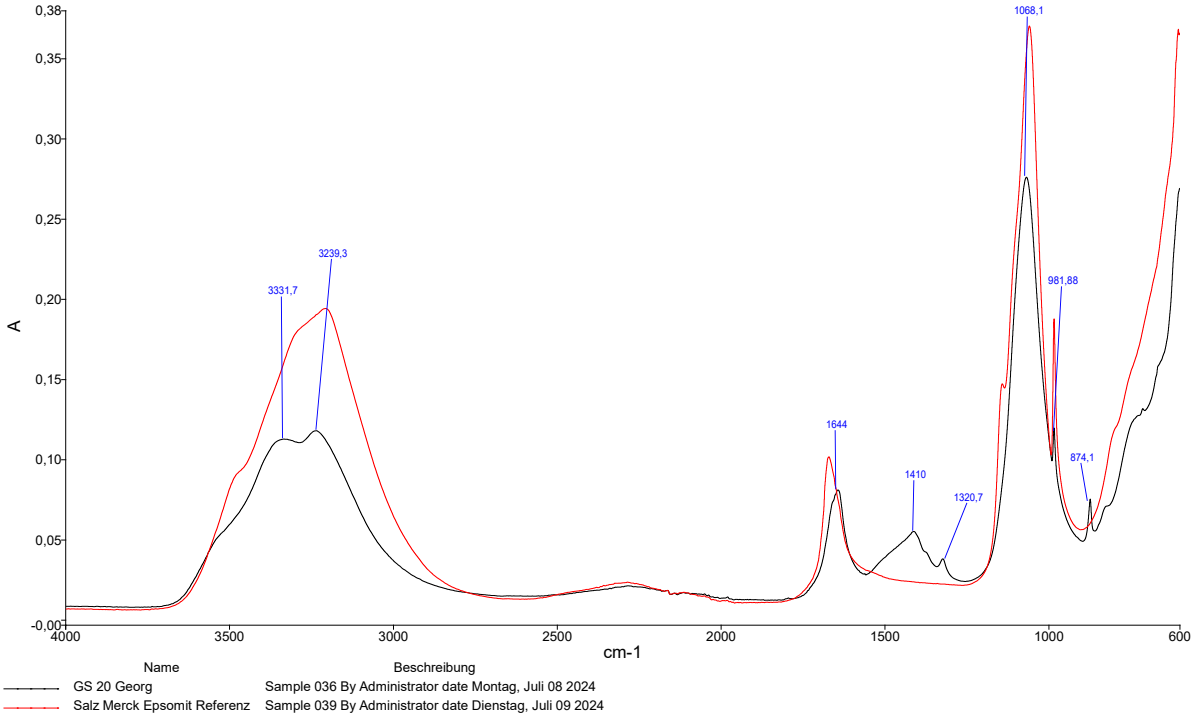

Fig. I-20: Sample 20, FTIR-spectra

Appendix I

Documentation of the measurements of salt efflorescences and crusts

Sample 21 – Location: NW chapel West Arch (Wa), 5

Description: white spots or postule (Fig. I-21).

Result by XRD: dypingite [$Mg_5(CO_3)_4(OH)_2 \bullet 5H_2O$] and lansfordite [$MgCO_3 \bullet 5H_2O$] (Fig. I-22).

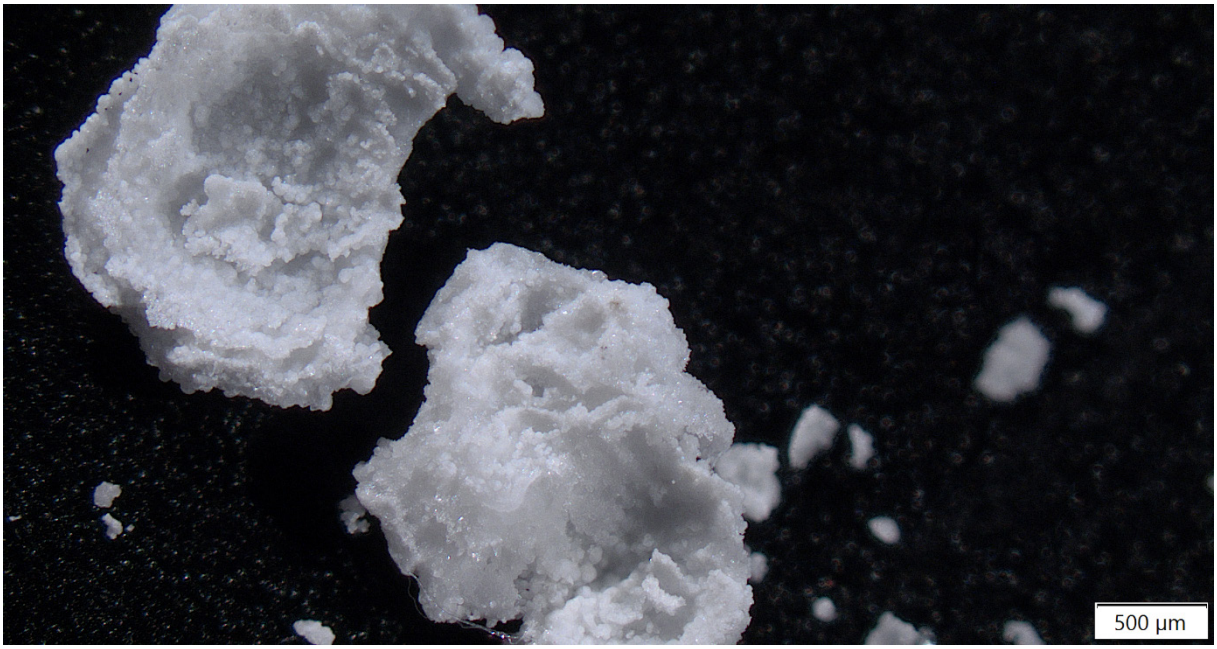

Fig. I-21: Sample 21: white spots or postule

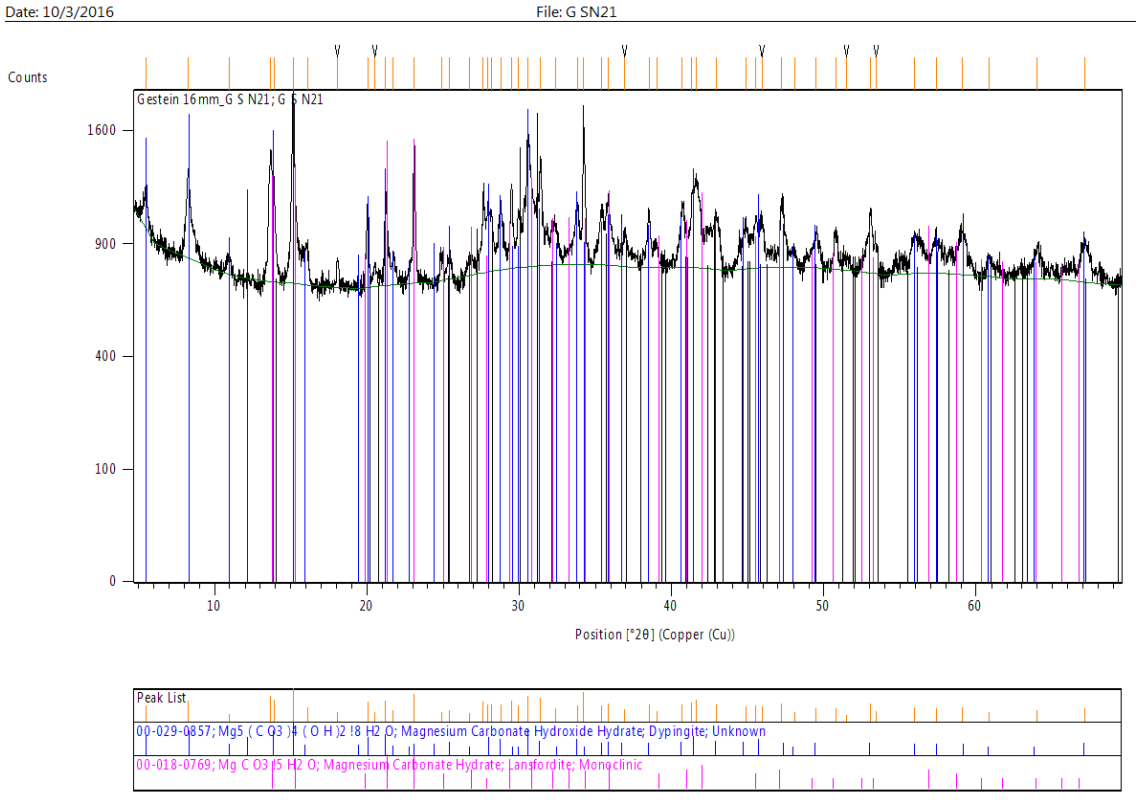

Fig. I-22: Sample 21, XRD spectrum

Appendix I

Documentation of the measurements of salt efflorescences and crusts

Sample 22 – Location: NW Chapel, North Wall, N10

Description: white flakes and transparent whisker (Fig. I-23).

Result by XRD: epsomite [$MgSO_4 \cdot 7H_2O$] and to a lower degree gypsum [$CaSO_4 \cdot 2H_2O$] (Fig.I-24).

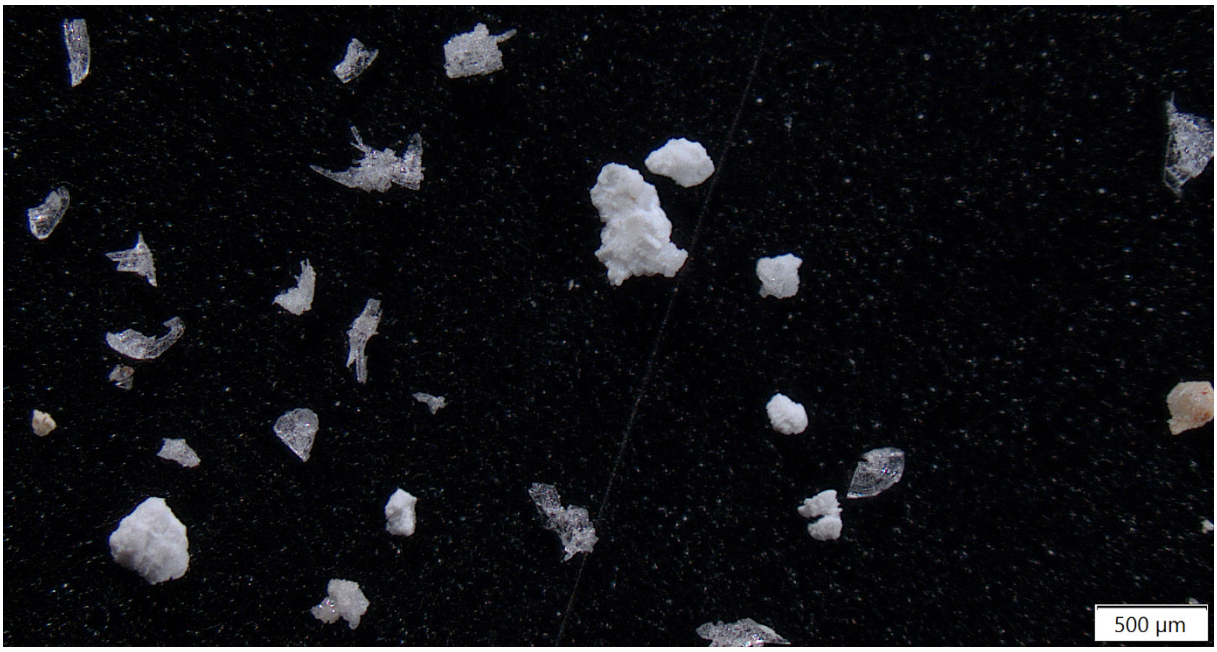

Fig. I-23: Sample 22: white flakes and transparent whisker

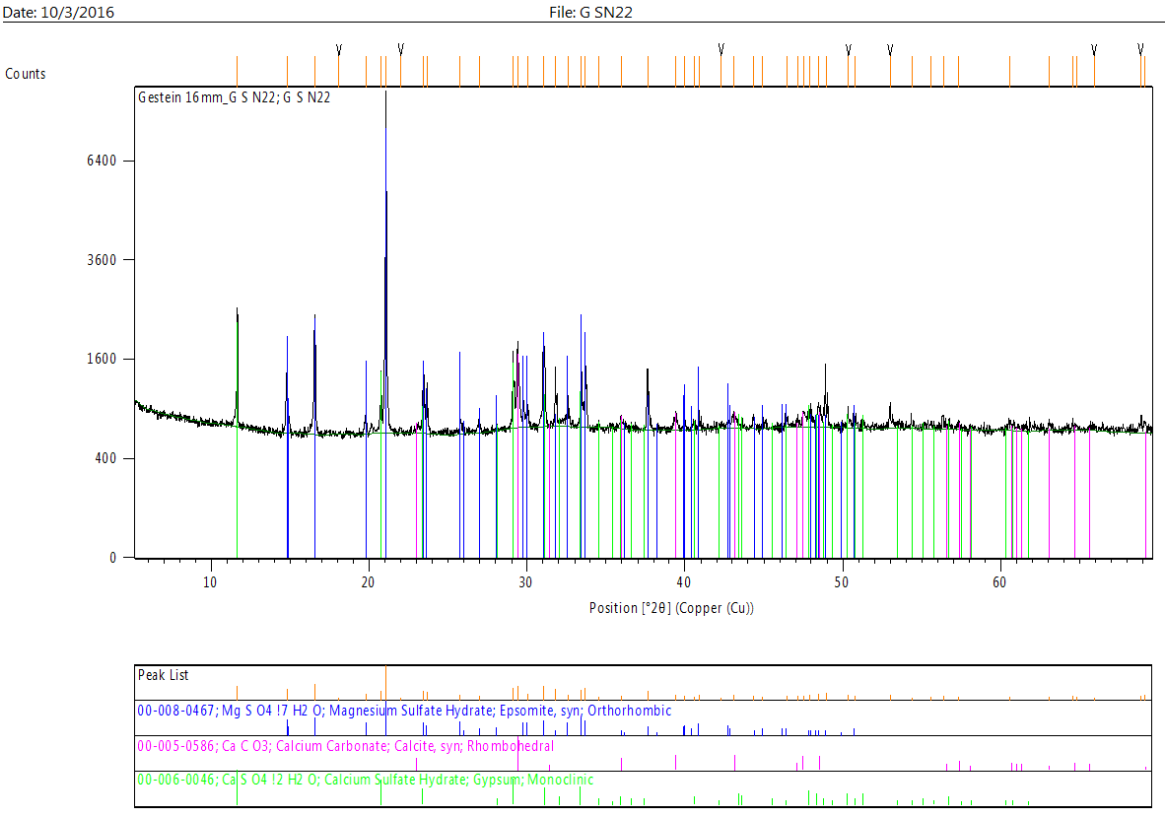

Fig. I-24: Sample 22, XRD spectrum

Appendix I

Documentation of the measurements of salt efflorescences and crusts

Sample 23 – Location: NW Chapel, NW Iconostasis

Description: granular crystals agglomerated to a crust (Fig. I-25).

Result by XRD: gypsum [$CaSO_4 \cdot 2H_2O$] (Fig.I-26).

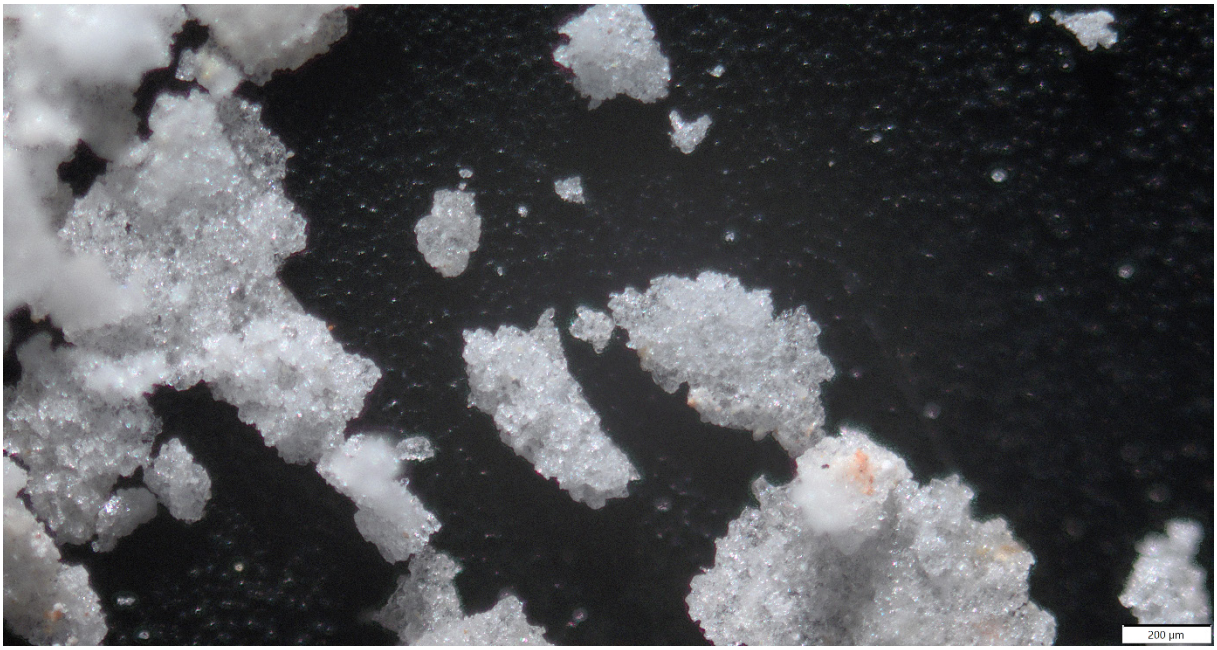

Fig. I-25: Sample 23: granular crystals agglomerated to a crust

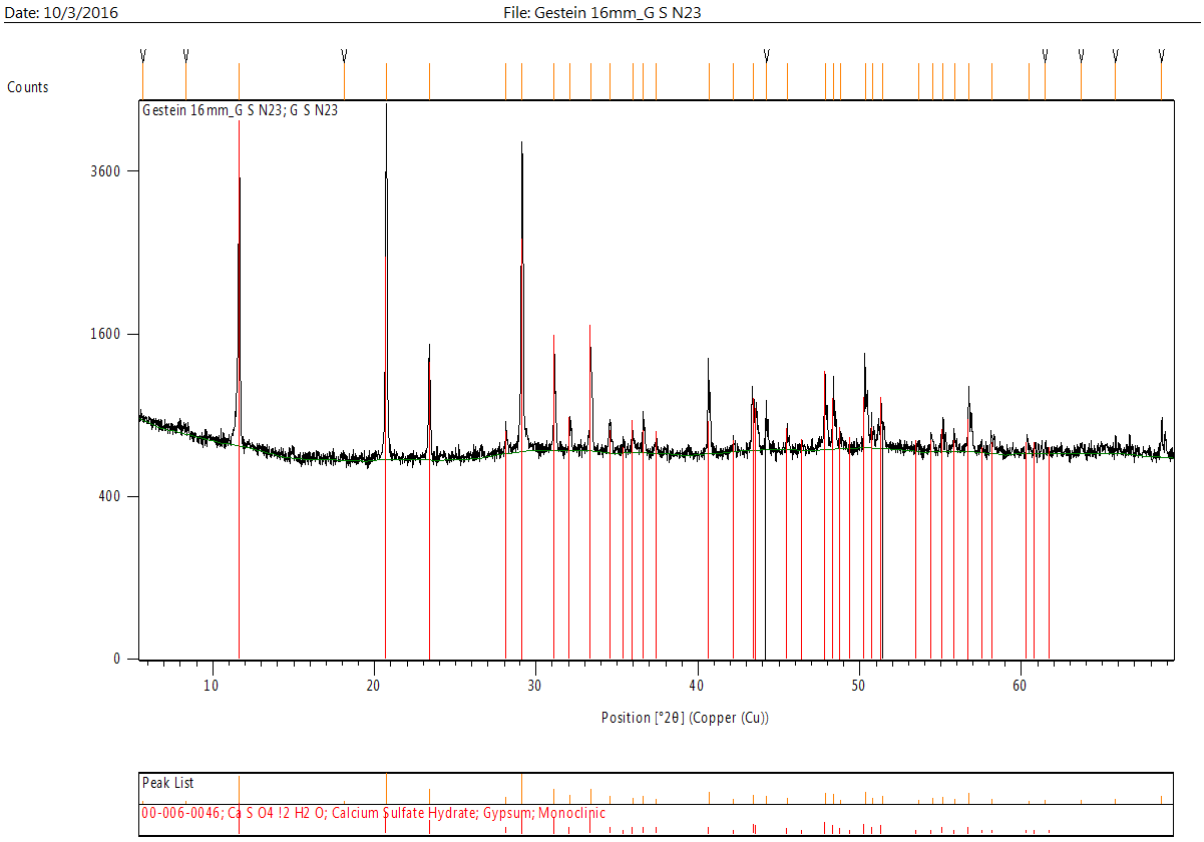

Fig. I-26: Sample 23, XRD spectrum

Appendix I

Documentation of the measurements of salt efflorescences and crusts

Sample 24 – Location: NW Chapel, South Wall, S7

Description: white granular crystals agglomerated to a crust (cauliflower crust) (Fig. I-27).

Result by XRD: hydromagnesite [$Mg_5(CO_3)_4(OH)_2 \cdot 4H_2O$] (Fig. I-28)

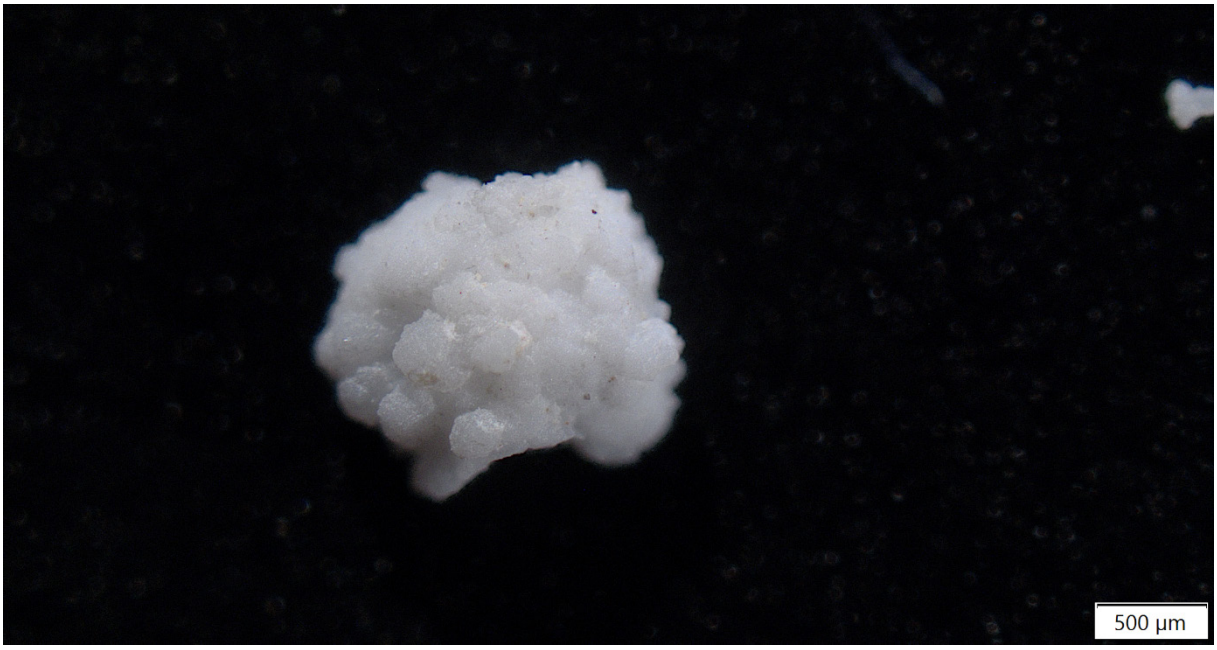

Fig. I-27: Sample 24: white granular crystals agglomerated to a crust, here cauliflower like

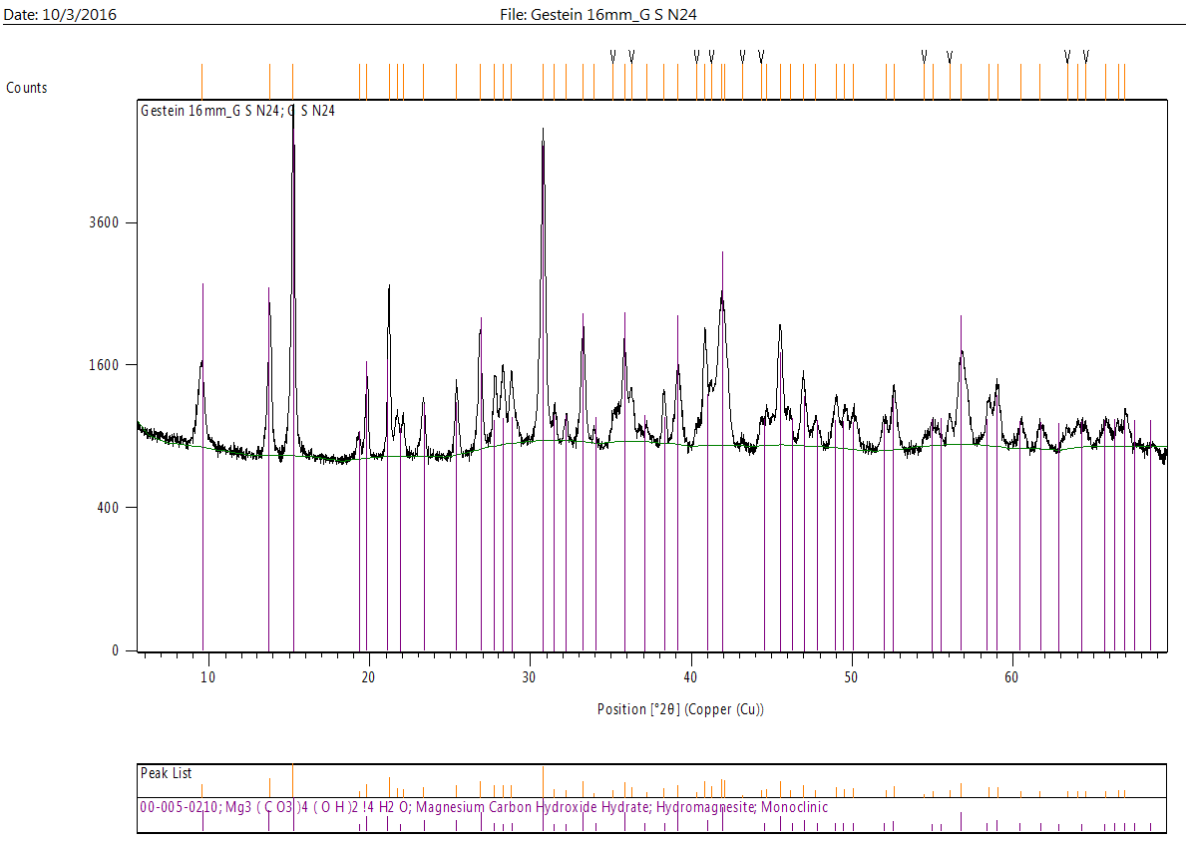

Fig. I-28: Sample 24, XRD spectrum

Appendix I

Documentation of the measurements of salt efflorescences and crusts

Sample 25 – Location: North Entrance (Ne), W5

Description: white granular crystals agglomerated to crust particles (Fig. I-29).

Result by XRD: calcite [$CaCO_3$] and to a lower degree gypsum [$CaSO_4 \cdot 2H_2O$] (Fig. I-30).

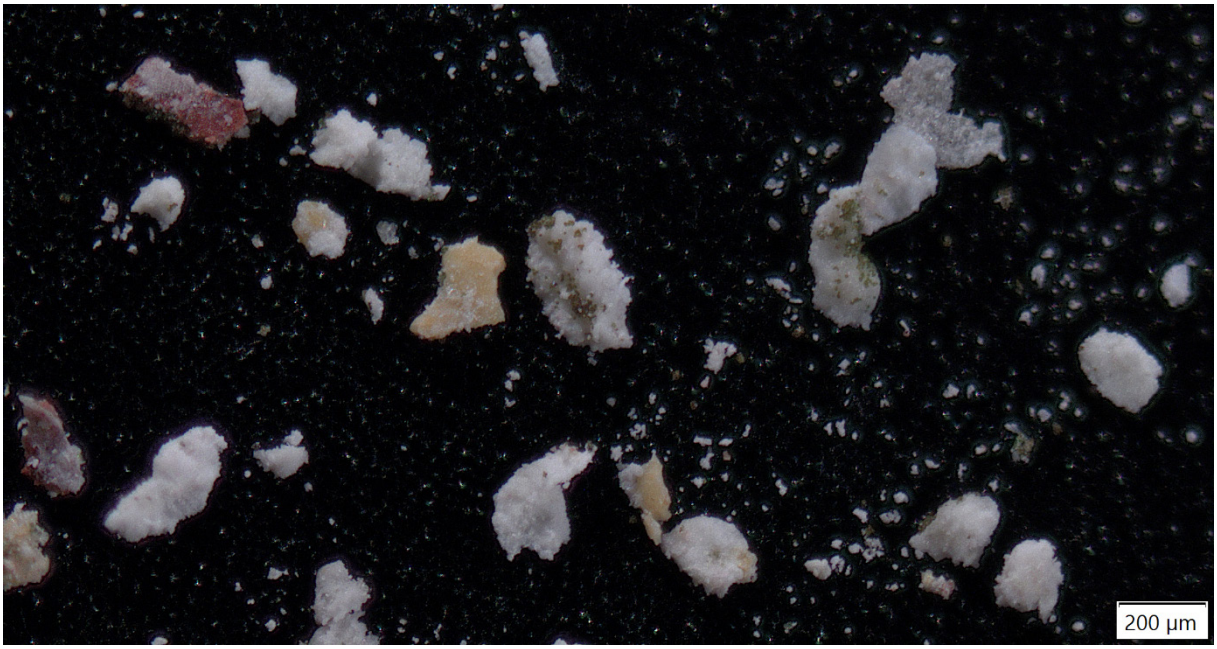

Fig. I-29: Sample 25: white granular crystals agglomerated to crust particles

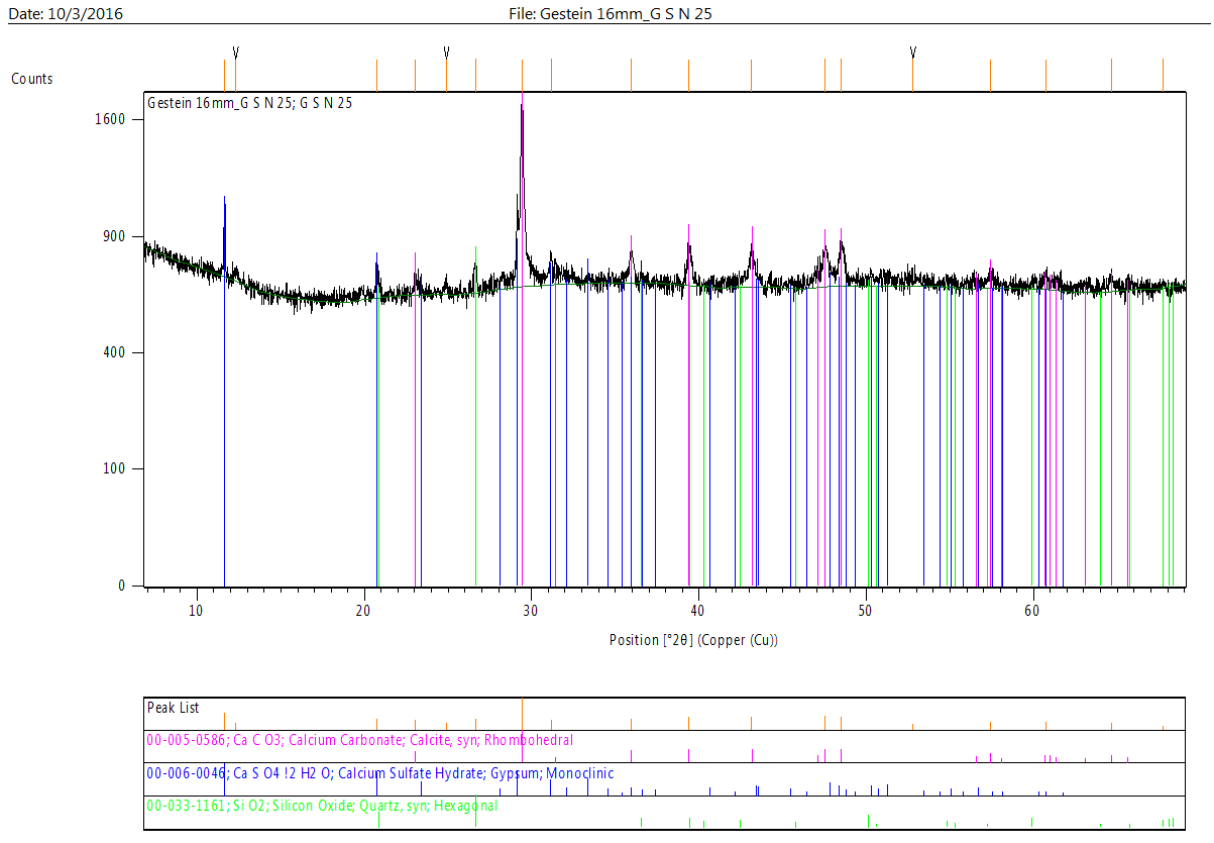

Fig. I-30: Sample 25, XRD spectrum

Appendix II

Data quantitative salt analyses e.c.= electric conductivity concentration in mass percent / weight percent [%w/w]

North Arm, East wall, II register, Scene E9 (Height: 16.7 m; from north wall: 0.5 m)					Na+	K+	Ca ++	Mg++	Cl-	NO3-	SO4--	sum
Sample	Depth [cm]	Material	e.c. [µS/cm]	pH-Value	[%w/w]	[%w/w]	[%w/w]	[%w/w]	[%w/w]	[%w/w]	[%w/w]	[%w/w]
Ne1_1	0,3	plaster	606	10,1	1,16	0,12	0,03	0,02	<0,01	0,02	0,06	1,42
Ne1_2	1	plaster	347	9,2	0,64	0,12	0,05	0,02	<0,01	0,02	0,04	0,89
Ne1_3	2	stone	93	7,9	0,06	0,05	0,09	0,04	<0,01	0,01	0,01	0,26
Ne1_4	4	stone	89	7,8	0,05	0,05	0,08	0,04	<0,01	0,01	0,01	0,23
Ne1_5	8	stone	94	7,8	0,05	0,04	0,09	0,04	<0,01	0,01	0,02	0,25
Ne1_6	14	stone	113	7,7	0,04	0,05	0,09	0,05	<0,01	0,01	0,02	0,26
Ne1_7	26	stone	117	7,8	0,03	0,05	0,10	0,07	<0,01	0,01	0,02	0,28
North Arm, East wall, III register, Scene E7 (Height: 13.4 m; from north wall: 0.6 m)												
Ne2_1	0,5	plaster	233	9,9	0,18	0,34	0,04	0,01	0,01	0,05	0,11	0,74
Ne2_2	1,5	stone	119	7,8	0,03	0,07	0,09	0,09	0,01	0,01	0,02	0,31
Ne2_3	3,5	stone	114	7,8	0,02	0,06	0,08	0,08	<0,01	0,01	0,02	0,27
Ne2_4	7,5	stone	98	7,7	0,02	0,03	0,07	0,07	<0,01	0,01	0,01	0,21
Ne2_5	13,5	stone	107	7,8	0,01	0,02	0,08	0,10	0,01	0,01	0,01	0,24
North Arm, East wall, IV register, Scene E5 (Height: 7.8 m; from north wall: 0.7 m)												
Ne3_1	0,5	plaster	1653	9,9	1,10	2,48	0,11	0,04	0,10	2,76	1,50	8,08
Ne3_2	1,5	stone	383	7,8	0,18	0,67	0,08	0,04	0,02	0,42	0,66	2,06
Ne3_3	3,5	stone	126	7,7	0,05	0,12	0,09	0,04	0,01	0,06	0,10	0,47
Ne3_4	7,5	stone	91	7,8	0,02	0,06	0,09	0,05	0,01	0,03	0,02	0,27
Ne3_5	13,5	stone	86	7,7	0,01	0,06	0,08	0,05	<0,01	0,01	0,02	0,23
Ne3_6	25,5	stone	80	7,7	0,01	0,04	0,09	0,05	<0,01	0,01	0,01	0,21
North Arm, West wall, III register, Scene W11 (Height: 12.1 m; from north wall: 0.9 m)												
Nw1_1	1	plaster	2192	9,9	2,40	2,41	0,11	0,04	0,08	2,42	0,94	8,40
Nw1_2	2	stone	374	7,8	0,42	0,46	0,05	0,03	0,02	0,35	0,23	1,56
Nw1_3	4	stone	141	7,8	0,09	0,16	0,08	0,04	0,02	0,09	0,03	0,51
Nw1_4	8	stone	97	7,7	0,04	0,09	0,09	0,04	0,01	0,04	0,02	0,32
Nw1_5	14	stone	86	7,8	0,02	0,06	0,07	0,04	0,01	0,01	0,01	0,22
Nw1_6a	26	stone	73	7,7	0,03	0,04	0,07	0,04	0,01	<0,01	0,01	0,20
Water extracts from other materials:												
Pumice			46	7,8	0,01	0,00	0,10	0,01	<0,01	0,01	0,02	0,16
filling mortar from 2018			69	7,1	0,01	0,01	0,14	0,01	<0,01	<0,01	0,02	0,20
Sw Pl 2.1	with straw	plaster	334	8,3	0,49	0,51	0,05	0,02	0,01	0,08	0,08	1,24
Sw Pl 2.2	black agg.	plaster	1062	10,6	1,19	1,22	0,07	0,02	0,04	0,23	0,56	3,31

Appendix II

Data quantitative salt analyses concentration in equivalent concentration [mEq/kg]

North Arm, East wall, II register, Scene E9 (Height: 16.7 m; f			Na+	K+	Ca ++	Mg++	Cl-	NO3-	SO4--	sum	ion balance	ion balance
Sample	Depth [cm]	Material	[mEq/kg]	[mEq/kg]	[mEq/kg]	[mEq/kg]	[mEq/kg]	[mEq/kg]	[mEq/kg]	[mEq/kg]	[mEq/kg]	[%]
Ne1_1	0,3	plaster	505	30	13	21	1	3	13	587	552	94
Ne1_2	1	plaster	278	31	23	14	1	3	9	359	332	93
Ne1_3	2	stone	27	12	43	30	1	1	3	117	107	91
Ne1_4	4	stone	21	12	38	29	1	1	3	105	95	90
Ne1_5	8	stone	22	11	43	34	1	1	3	116	105	90
Ne1_6	14	stone	19	13	43	44	1	1	4	125	113	91
Ne1_7	26	stone	15	12	48	57	1	2	3	139	126	90
North Arm, East wall, III register, Scene E7 (Height: 13.4 m; from north wall: 0.6 m)												
Ne2_1	0,5	plaster	77	88	21	10	2	9	22	229	164	72
Ne2_2	1,5	stone	11	19	43	72	2	2	4	154	137	89
Ne2_3	3,5	stone	10	14	39	64	1	2	4	134	120	89
Ne2_4	7,5	stone	7	8	37	55	1	1	2	112	103	92
Ne2_5	13,5	stone	5	6	39	83	2	1	3	138	128	92
North Arm, East wall, IV register, Scene E5 (Height: 7.8 m; from north wall: 0.7 m)												
Ne3_1	0,5	plaster	477	633	56	30	29	444	312	1982	411	21
Ne3_2	1,5	stone	78	171	40	33	5	68	137	531	112	21
Ne3_3	3,5	stone	24	30	44	32	4	10	20	164	96	59
Ne3_4	7,5	stone	10	15	44	40	3	4	4	119	97	81
Ne3_5	13,5	stone	6	14	39	40	1	2	4	107	92	86
Ne3_6	25,5	stone	5	10	43	42	1	1	2	105	96	92
North Arm, West wall, III register, Scene W11 (Height: 12.1 m; from north wall: 0.9 m)												
Nw1_1	1	plaster	1046	616	55	31	23	391	196	2357	1138	48
Nw1_2	2	stone	185	118	25	22	6	57	47	460	240	52
Nw1_3	4	stone	40	40	42	32	4	15	7	181	128	71
Nw1_4	8	stone	18	22	46	32	3	7	4	130	105	80
Nw1_5	14	stone	8	15	37	30	2	2	2	96	85	88
Nw1_6a	26	stone	14	11	37	31	1	<1	1	96	90	94
Water extracts from other materials:												
Pumice			3	1	51	12	0	1	5	72	61	84
filling mortar from 2018			5	3	71	7	0	<1	5	92	80	87
Sw Pl 2.1	with straw	plaster	215	130	26	17	2	13	17	420	357	85
Sw Pl 2.2	black agg.	plaster	516	311	33	14	11	36	116	1037	711	137

Appendix III

Plaster analyses by XRD

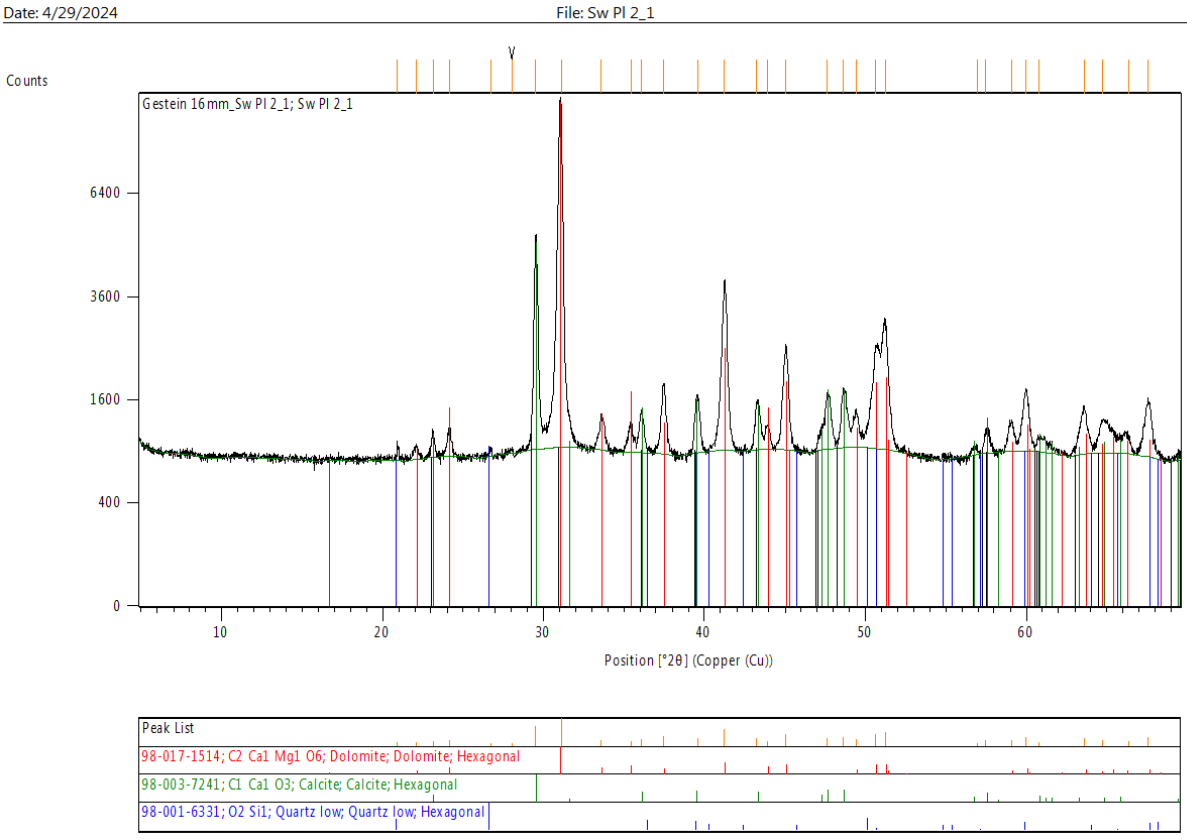

Fig. III-1: Sample Sw Pl 2_1, XRD spectrum: more dolomite than calcite

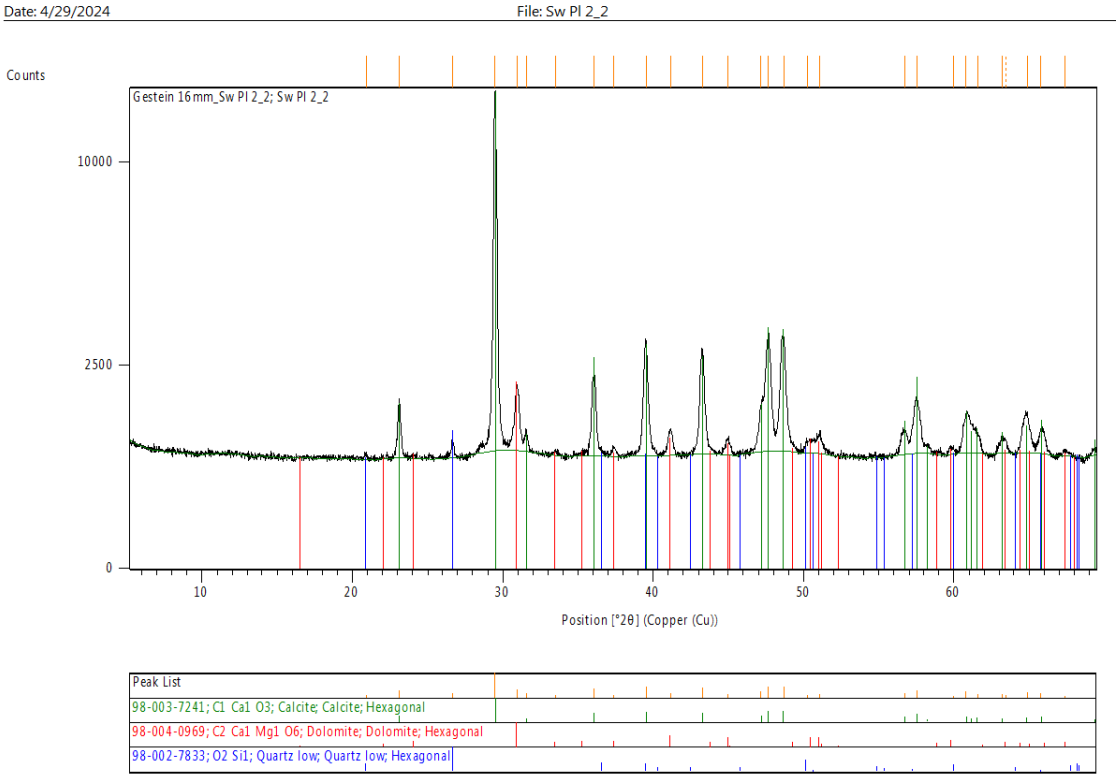

Fig. III-2: Sample Sw Pl 2_2, XRD spectrum: much more calcite than dolomite

Appendix III

Plaster analyses by XRD

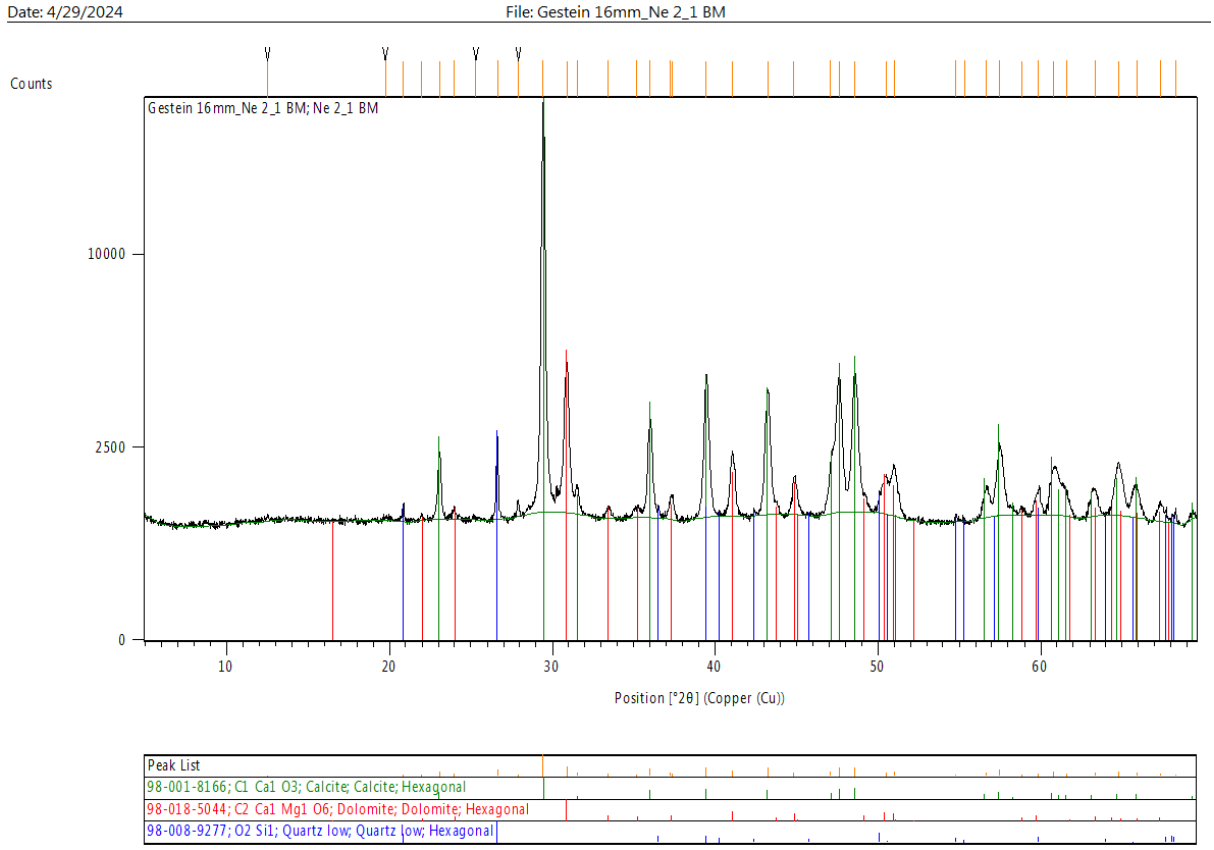

Fig. III-3: Sample Ne 2_1, XRD spectrum: more calcite than dolomite

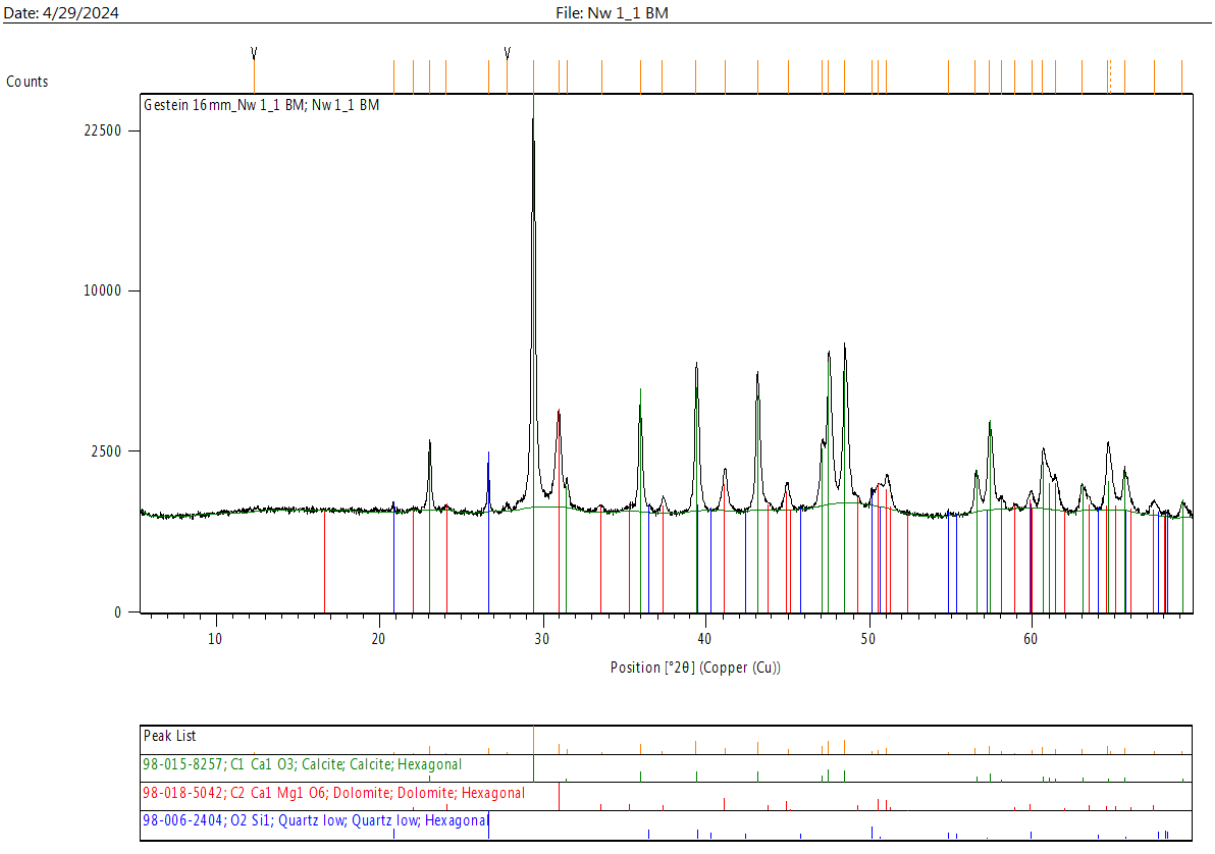

Fig. III-4: Sample Nw 1_1, XRD spectrum: more calcite than dolomite